98°C for 10 sec, 60°C for 30 sec, and 68°C for 1 min for 35 cycles in an automated thermal cycler (GeneAmp PCR System 9700; Applied Biosystems Foster City, CA, USA). The PCR products were purified with Wizard SV Gel and PCR Clean-up System (Promega, Madison, WI, USA) or treated with Exonuclease I and Antarctic Phosphatase (New England Biolabs, Ipswich, MA, USA). Direct sequencing was performed with the BigDye Terminator v3.1 Cycle Sequencing Kit on an ABI3100 autosequencer (Applied Biosystems, Foster City, CA, USA).

RESULTS

Clinical Findings

At the first visit in 1986 when she was 6 years old, her VA was 1.0 in both eyes without correction, and her refractive errors were +2.50 diopters (D) = −1.25D × 180° in the right eye and +1.50D = −0.50D × 180° in the left eye. The visual fields determined by Goldmann perimeter were full, and the anterior segments determined by slit-lamp microscopic examination were normal (Fig. 1A & B). Ophthalmoscopy showed many small white dots in the posterior pole of both eyes in 1986 and 2003 (Fig. 2A & B, photographs from 2003). She was diagnosed with atypical fundus albipunctatus. The course of both the cone and rod dark-adaptation was abnormal. The color vision determined by the Ishihara chart in 1999 showed that the patient was not able to detect the numbers in 21 plates. The Panel D-15 test performed in 1999 showed color vision defect in both eyes.

The vision disturbances and central scotomas in both eyes were first detected when the patient was in her twenties (Fig. 1C & D).

At 30 years of age, changes in the retinal pigment epithelium (RPE) were observed in both eyes (Fig. 2C & D).Fluorescein angiography was performed in 2010 (Fig. 2E & F), and a diffuse hyperfluorescence was seen in the macular area in the early arteriovenous phase. A granular type hyperfluorescence corresponding to the atrophic area appeared outside the vascular arcades.

Nowadays she is 31 years old and her BCVA is 0.1 OD and 0.5 OS and her refraction are +0.50D = −3.00D × 170° in the right eye and +1.00D = −3.50D × 10° in the left eye.

Optical coherence tomography (OCT) showed a generalized retinal thinning in the central foveal area (Fig. 2G & H).

Electrophysiological Analyses

Representative full-field ERGs are shown in Fig. 3. When the patient was 7 years old, the rod response was undetectable, and the amplitude of the single-flash cone response and 30-Hz flicker response were reduced by about 50% (Fig. 3A). The maximal rod-cone response after 30 min of dark-adaptation was also severely reduced but was still detectable (Fig. 3B, right column). The amplitudes of the ERGs decreased with increasing

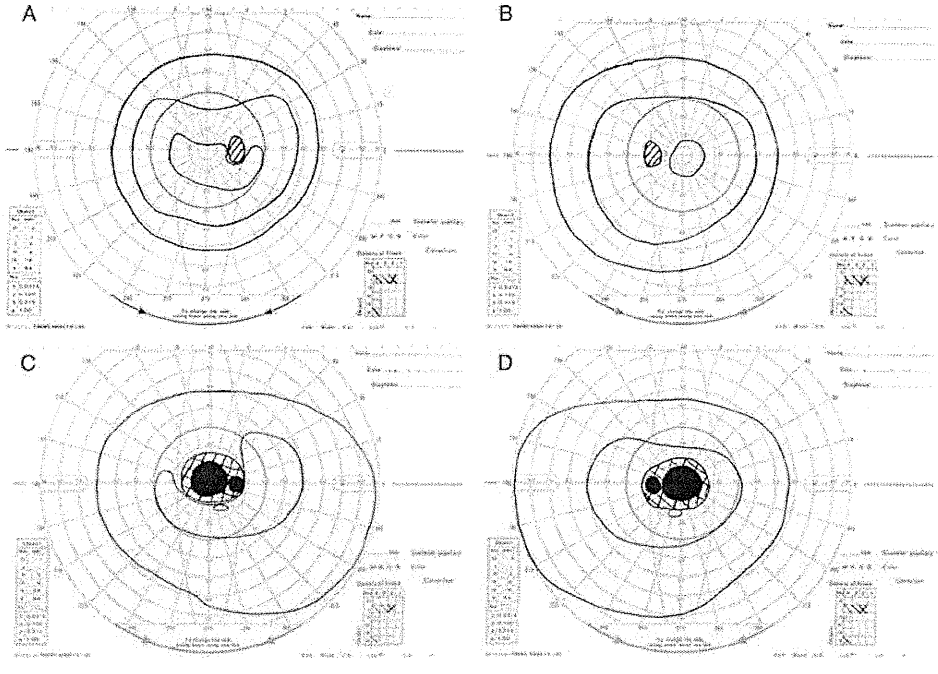

FIGURE 1 Progression of visual field defects in a patient with Bothnia dystrophy. (A and B) Left eye (A) and right eye (B) at age 6 years. Visual fields are essentially normal in both eyes. (C and D) Left eye (C) and right eye (D) at age 30 years. Central scotoma is present in both eyes.

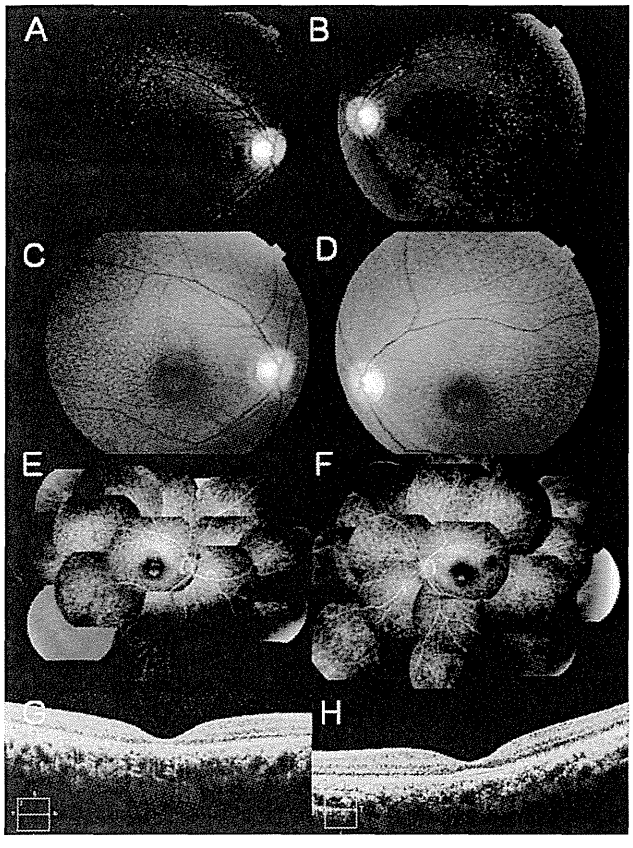

FIGURE 2 Fundus photographs of a patient with Bothnia dystrophy. (A and B) Fundus photograph of the right (A) and left (B) eyes taken at age 23 years. (C and D) Fundus photograph of the right (C) and left (D) eyes taken at age 30 years. Numerous tiny white dots can be seen in both eyes. Changes in the RPE can be seen at age 30 years old in both eyes. (E and F) Fluorescein angiograms of the right eye (E) and left eye (F) taken at age 30 years. The early arteriovenous phase shows a diffuse hyperfluorescence in the macular area. (G and H) Right Cross sectional optical coherence tomographic images of the right (G) and left (H) eyes taken at age 31 years. Retinal thinning can be seen.

age and were almost undetectable when she was 32 years old.

To examine whether these reduced ERG responses were due to a delay of dark-adaptation we recorded the maximal rod-cone ERGs after prolonged dark-adaptation. The amplitude of maximal rod-cone ERG did not increase after 3 hrs dark-adaptation (Fig. 3C, upper trace), but increased by approximately three fold after 24 hrs of dark-adaptation (Fig. 3C, middle trace) when she was 7 years old. This phenomenon was also confirmed when she was 32 years old. The nearly undetectable maximal rod-cone ERG became clearly detectable at 95 μV after 24 hrs of dark-adaptation (Fig. 3C, lower trace).

Mutation Analyses

Although no mutation was detected in the *RDH5* and rhodopsin genes, a homozygous R234W mutation was detected in the *RLBP1* gene (data not shown).

DISCUSSION

We initially diagnosed our patient with an atypical variant of fundus albipunctatus instead of RPA because the mixed rod-cone response recovered significantly after 24 hrs of dark-adaptation. But the visual disturbances and visual field scotomas appeared in her twenties. At that age, the BCVA was also depressed. Recent investigations of patients with fundus albipunctatus caused by a *RDH5* gene mutation showed that the retinal changes were not stationary and frequently progressed to cone dystrophy in their fifties.[17] Genetic analyses showed a *RLBP1* gene mutation instead of a *RDH5* gene mutation confirming our diagnosis of RPA.

RLBP1 gene mutations cause autosomal recessive retinitis pigmentosa (RP), RPA, fundus albipunctatus, and Newfoundland rod-cone dystrophy.[9,13,14] Known allelic variants of the *RLBP1* gene now include missense mutations, frameshift mutations that result in truncation, and canonical splice donor site mutations that prevent translation of the protein. Our case is the second report of a *RLBP1* mutation in a Japanese patient with the RPA phenotype. The number of patients with RPA seems to be fewer than those with fundus albipunctatus in Japan. The other Japanese case with the *RLBP1* mutation was due to compound heterozygous mutations of R103W and R234W and had the RPA phenotype.[18]

The atypical variant of autosomal recessive retinitis pigmentosa (RP) was known to clinicians in northern Sweden for decades as Västerbotten dystrophy or BD and has been well characterized.[19–21] BD patients have night blindness from early childhood, followed by macular degeneration and a decrease in visual acuity that lead to legal blindness in early adulthood. The disorder has been associated with a missense mutation, R234W, in the *RLBP1* gene. Because we detected a homozygous R234W mutation, this is the first non-Swedish patient with BD if the gene mutation determined the disease nomenclature. To support this, our case had the typical clinical features described for BD patients.

Although the parents of our case are not relatives, consanguinity might be suspected because her parent's ancestors lived in adjacent areas. In 1999, Morimura[9] reported that a patient who was a member of Swedish pedigree had a homozygous R234W mutation. Because the R234W mutation is not widespread in the world, we suggest that this R234W mutation most likely represents a recurrent mutation rather than a founder mutation of Swedish origin. The R234W mutation is caused by single base substitution from CGG to TGG. Methylated CpG sequences frequently undergo mutation resulting in single base substitution because deamination of 5-methylcytosines easily forms thymine. This conversion of a DNA base from cytosine to thymine within the coding regions can result in a pathogenic mutation. In human genetic diseases, methylated CpG sequences are mutational hotspots.[22] Thus, the Japanese R234W

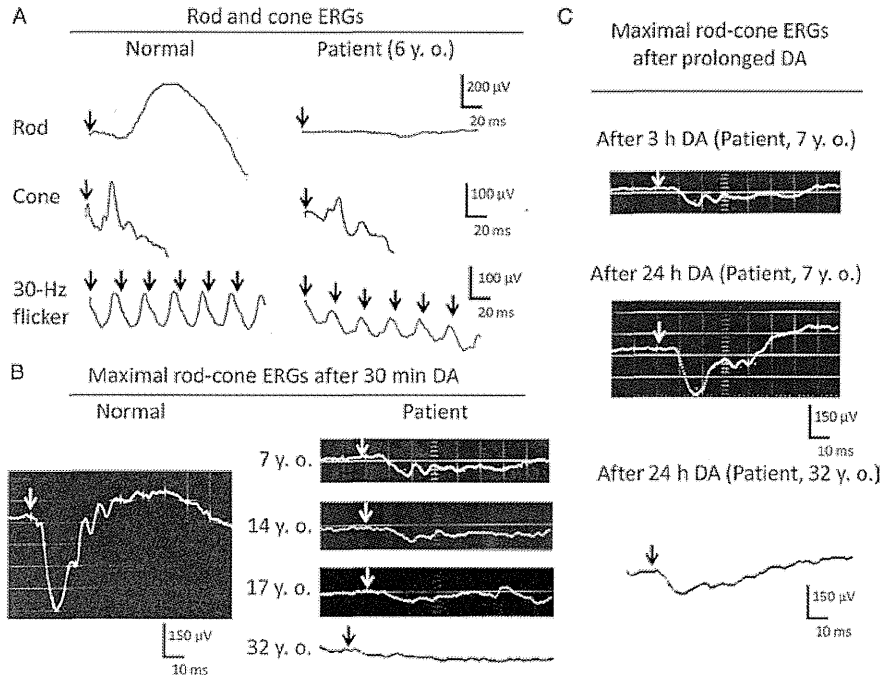

FIGURE 3 Full-field electroretinograms (ERGs) recorded from a patient with Bothnia dystrophy. (A) Rod and cone ERGs recorded from a normal subject (left) and our patient at age 6 years. Arrowheads indicate the onset of the flash stimulus. Rod responses, single-flash cone responses, and 30-Hz flicker ERGs are shown. (B) Maximal rod-cone ERGs recorded after 30 min of dark-adaptation from a normal subject (left) and our patient at ages 7, 14, 17, and 32 years (right). The ERG amplitudes of our patient decrease with increasing age. (C) Maximal rod-cone ERG responses recorded from our patient after different durations of dark-adaptation. Maximal rod-cone ERG after 3 hrs of dark-adaptation (upper trace) and after 24-hr dark-adaptation (middle trace) when the patient was 7 years old. Maximal rod-cone ERG after 24-hr dark-adaptation recorded from our patient when she was 32 years old (lower trace).

mutation may have occurred at the methylated CpG sequence. Three of the four *RLBP1* gene mutated alleles in Japanese RPA patients are R234W. We could not determine if the R234W mutation in those Japanese RPA patients has a founder effect from a Japanese ancestor or occurred independently. A linkage analysis study on the *RLBP1* locus haplotypes from those patients will be performed in the future to clarify the possibility of a common ancestor.

ACKNOWLEDGMENTS

This study was supported by research grants from the Ministry of Health, Labour and Welfare (Research on Measures for Intractable Diseases) and from Japan Society for the Promotion of Science (Grant-in-Aid for Scientific Research (C) 23592561 and Grant-in Aid for Young Scientists (B) 23791975).

Declaration of interest: The authors report no conflicts of interest. The authors alone are responsible for the content and writing of the paper.

REFERENCES

1. Sabel Aish SF, Dajani B. Benign familial fleck retina. Br J Ophthalmol 1980;64:652–659.
2. Yamamoto H, Simon A, Eriksson U, et al. Mutations in the gene encoding 11-cis retinol dehydrogenase cause delayed dark adaptation and fundus albipunctatus. Nat Genet 1999;22:188–191.
3. Nakamura M, Hotta Y, Tanikawa A, et al. A high association with cone dystrophy in fundus albipunctatus caused by mutations of the *RDH5* gene. Invest Opthalmol Vis Sci 2000;41:3925–3932.
4. Driessen CA, Janssen BP, Winkens HJ, et al. Null mutation in the human 11-cis retinol dehydrogenase gene associated with fundus albipunctatus. Ophthalmology 2001;108:1479–1484.
5. Hotta K, Nakamura M, Kondo M, et al. Macular dystrophy in a Japanese family with fundus albipunctatus. Am J Ophthalmol 2003;135:917–919.
6. Katsanis N, Shroyer NF, Lewis RA, et al. Fundus albipunctatus and retinitis punctata albescens in a pedigree with an R150Q mutation in *RLBP1*. Clin Genet 2001;59:424–429.
7. Kajiwara K, Sandberg MA, Berson EL, et al. A null mutation in the human peripherin/RDS gene in a family with autosomal dominant retinitis punctata albescens. Nat Genet 1993;3:208–212.
8. Souied E, Soubrane G, Benlian P, et al. Retinitis punctata albescens associated with the Arg135Trp mutation in the rhodpsin gene. Am J Ophthalmol 1996;121:19–25.
9. Morimura H, Berson EL, Dryja TP. Recessive mutations in the *RLBP1* gene encoding protein in a form of retinitis punctata albescens. Invest Opthalmol Vis Sci 1999;40:1000–1004.
10. Fishman GA, Roberts MF, Derlacki DJ, et al., Novel mutations in the cellular retinaldehyde-binding protein gene (RPBP1) associated with retinitis punctata albescens. Arch Ophthalmol 2004;122:70–75.
11. Humbert G, Delettre C, Sénéchal A, et al. Homozygous deletion related to Alu repeats in *RLBP1* causes retinitis punctata albescens. Invest Ophthalmol Vis Sci 2006;47:4719–4724.

12. Singh HP, Jalali S, Narayanan R, et al. Genetic analysis of Indian families with autosomal recessive retinitis pigmentosa by homozygosity screening. Invest Ophthalmol Vis Sci 2009;50:4065–4071.
13. Maw MA, Kennedy B, Knight A, et al. Mutation of the gene encoding cellular retinaldehyde-binding protein in autosomal recessive retinitis pigmentosa. Nat Genet 1997;17:198–200.
14. Eichers ER, Green JS, Stockton DW, et al. Newfoundland rod-cone dystrophy, an early-onset retinal dystrophy, is caused by splice-junction mutation in *RLBP1*. Am J Hum Genet 2002;70:955–964.
15. Burstedt MS, Sandgren O, Holmgren G, et al. Bothnia dystrophy caused by mutations in the cellular retinaldehyde-binding protein gene (*RLBP1*) on chromosome 15q26. Invest Ophthalmol Vis Sci 1999;40:995–1000.
16. Wang C, Nakanishi N, Ohishi K, et al. Novel *RDH5* mutation in family with mother having fundus albipunctatus and three children with retinitis pigmentosa. Ophthalmic Genet 2008;29:29–32.
17. Nakamura M, Skalet J, Miyake Y. *RDH5* gene mutations and electroretinogram in fundus albipunctatus with or without macular dystrophy. Doc Opthalmol 2003;107:3–11.
18. Nakamura M, Lin J, Ito Y, et al. Novel mutation in *RLBP1* gene in a Japanese patient with retinitis punctata albescens. Am J Ophthalmol 2005;139:1133–1135.
19. Burstedt MS, Forsmann-Semb K, Golovleva I, et al. Ocular phenotype of Bothnia dystrophy, an autosomal recessive retinitis pigmmentosa associated with an R234W mutation in the *RLBP1* gene. Arch Ophthalmol 2001;119:260–267.
20. Burstedt MS, Sandgren O, Golovleva I. Effect of prolonged dark adaptation in patients with retinitis pigmentosa of Bothnia type: an electrophysiological study. Doc Ophthalmol 2008;116:193–205.
21. Burstedt MS, Golovleva I. Central retinal finding in Bothnia dystrophy caused by *RLBP1* sequence variation. Arch Ophthalmol 2010;128:989–995.
22. Sved J, Bird A. The expected equilibrium of the CpG dinucleotide in vertebrate genomes under a mutation model. Proc Natl Acad USA 1990;87:4692–4696.

Photoreceptor and Post-Photoreceptoral Contributions to Photopic ERG a-Wave in Rhodopsin P347L Transgenic Rabbits

Rika Hirota,[1,2] *Mineo Kondo,*[3] *Shinji Ueno,*[1] *Takao Sakai,*[1] *Toshiyuki Koyasu,*[1] *and Hiroko Terasaki*[1]

Purpose. The a-wave of the photopic electroretinogram (ERG) of macaque monkeys is made up of the electrical activities of cone photoreceptors and post-photoreceptoral neurons. However, it is not known whether the contributions of these two components change in retinas with inherited photoreceptor degeneration. The purpose of this study was to determine the contributions of cones and post-photoreceptoral neurons to the a-wave of the photopic ERGs in rhodopsin Pro347Leu transgenic (Tg) rabbits.

Methods. Ten Tg and 10 wild-type (WT) New Zealand White rabbits were studied at 4 and 12 months of age. The a-waves of the photopic ERGs were elicited by xenon flashes of different stimulus strengths before and after the activities of post-photoreceptoral neurons were blocked by intravitreal injections of a combination of 0.2 to 0.4 mM of 6-cyano-7-nitrouinoxaline-2,3(1H,4H)-dione, disodium (CNQX) and 2 to 4 mM of (±)-2-amino-4-phosphonobutyric acid.

Results. The percentage contribution of the cone photoreceptors to the photopic ERG a-waves increased with increasing stimulus strength, and the percentage ranged from 54% to 75% in 4-month-old WT rabbits. In contrast, the percentage contribution of the cone photoreceptors in 4-month-old Tg rabbits ranged from 32% to 51% ($P < 0.05$). The mean percentage contribution of cone photoreceptors became still smaller at 11% to 48% in 12-month-old Tg rabbits.

Conclusions. These results suggest that the relative contribution of cone photoreceptors to the photopic ERG a-wave is smaller in retinas with inherited photoreceptor degeneration. This indicates that the a-waves of the photopic ERGs in patients with retinitis pigmentosa must consider this lower contribution from the cone photoreceptors. (*Invest Ophthalmol Vis Sci.* 2012;53:1467–1472) DOI:10.1167/iovs.11-9006

The electroretinogram (ERG) is a mass electrical potential change of the retina that is elicited by light stimulation and is easily recorded noninvasively with a corneal electrode.[1] The ERG arises from the neural activity of the different types of retinal cells, and it can be used to perform a layer-by-layer study of retinal function in patients and animals.[2]

The origins of the photopic or light-adapted a-wave of the ERG in macaque monkeys was studied by Sieving et al.[3–5] They injected glutamate agonists and antagonists intravitreally to dissect the retinal circuits. They found that the a-wave of the photopic ERG received contributions not only from the cone photoreceptors but also from post-photoreceptoral neurons (e.g., OFF-bipolar cells and horizontal cells)[3,4] because *cis*-2,3-piperidine dicarboxylic acid (PDA) or kynurenic acid reduced the a-wave amplitude. A later study by Robson et al.[6] showed that the PDA-sensitive post-photoreceptoral a-wave component started at much earlier times of approximately 5 ms in macaques. Frieberg et al.[7] also estimated the time course of the cone photoreceptor response in normal human ERGs using the paired-flash technique, in which an intense "probe" flash was delivered at different times after a "test" flash. Their results showed that the photopic ERG a-wave of the human ERG contains an appreciable postphotoreceptoral component, similar to that reported in monkeys.[3–6]

These studies, which were designed to determine the origins of the photopic ERG a-wave, have been performed primarily on normal macaque monkeys and human eyes.[3–7] It is not known whether the contributions of photoreceptors and post-photoreceptoral neurons are altered in retinas with inherited photoreceptor degeneration (e.g., retinitis pigmentosa [RP]) because the most commonly used RP animals are mice and rats, whose amplitude of photopic ERG a-wave is very small. This makes it difficult to quantify the changes in the a-wave amplitude before and after intravitreal injection of pharmacologic agents.[8–12]

We have recently succeeded in generating a rabbit model of retinal degeneration.[13] This animal has the rhodopsin Pro347Leu mutation, which is one of the major mutations in autosomal dominant retinitis pigmentosa in humans.[14] These animals have a slowly progressive photoreceptor degeneration, as do human RP patients with this mutation,[13,15–18] though it is still unclear whether the retinal degeneration is due to a point mutation of the rhodopsin gene or to an overexpression of rhodopsin in these animals. We believed that this rhodopsin transgenic (Tg) rabbit can be an excellent animal model in which to study the retinal origins of the photopic ERG a-wave in RP because rabbits have a large photopic a-wave. In addition, the large size of the rabbit's eye enabled us to perform reliable intravitreal injections of pharmacologic agents.[15,16,18]

Thus, the purpose of this study was to compare the contributions of cone photoreceptors and post-photoreceptoral neurons with the a-wave of the photopic ERGs between wild-type (WT) and Tg rabbits. To accomplish this we examined the postphotoreceptoral neural activity before and after they were blocked by pharmacologic agents.

From the [1]Department of Ophthalmology, Nagoya University Graduate School of Medicine, Nagoya, Japan; the [2]Drug Safety Research Laboratories, Astellas Pharma Inc., Osaka, Japan; and the [3]Department of Ophthalmology, Mie University Graduate School of Medicine, Tsu, Japan.

Supported by Grant-in-Aid for Scientific Research B (203904480) and Grant-in-Aid for Scientific Research C (20592075) from the Ministry of Education, Culture, Sports, Science and Technology, Japan.

Submitted for publication November 3, 2011; revised January 13, 2012; accepted January 14, 2012.

Disclosure: **R. Hirota**, Astellas Pharma Inc. (E); **M. Kondo**, None; **S. Ueno**, None; **T. Sakai**, None; **T. Koyasu**, None; **H. Terasaki**, None

Corresponding author: Mineo Kondo, Department of Ophthalmology, Mie University Graduate School of Medicine, 2-174 Edobashi, Tsu 514-8507, Japan; mineo@clin.medic.mie-u.ac.jp.

Materials and Methods

Animals

The experiments were performed on 10 Tg and 10 littermate WT New Zealand White rabbits. Our techniques for generating Tg rabbits have been described in detail.[13] This study was conducted in accordance with the ARVO Statement for the Use of Animals in Ophthalmic and Vision Research. All protocols were approved by the Animal Research Review Board of Nagoya University Graduate School of Medicine (no. 23005).

ERG Recordings

Each animal was anesthetized with an intramuscular injection of 25 mg/kg ketamine and 2 mg/kg xylazine. ERGs were recorded with a bipolar contact lens electrode (GoldLens; Doran Instruments, Littleton, MA). Animals were placed in a Ganzfeld bowl and stimulated with stroboscopic stimuli (model SG-2002; LKC Technologies, Gaithersburg, MD). The full-strength stimulus was attenuated with neutral density filters in 0.5-log unit steps. Photopic ERGs were recorded after 10 minutes of light adaptation, and the stimulus strength ranged from 0.2 to 2.2 log cd-s/m^2 (photopic unit), and they were presented on a rod-suppressing white background of 3.3 log scot td. Signals were amplified, band pass-filtered between 0.3 to 1000 Hz, and averaged using a computer-assisted signal analysis system (MEB-9100; Neuropack, Nihon Kohden, Tokyo, Japan).

Drug Injections

Drugs and techniques for the intravitreal injections have been described in detail.[15,16,18] The drugs were dissolved in sterile PBS, and the pH was titrated to 7.4 with hydrochloric acid or sodium hydrate. The drugs were injected into the vitreous with a 30-gauge needle inserted through the pars plana approximately 1 mm posterior to the limbus.

Two types of glutamate analogs—(±)-2 amino-4-phosphonobutyric acid (APB; Sigma-Aldrich Japan, Tokyo, Japan) and 6-cyano-7-nitroquinoxaline-2,3(1H,4H)-dione (CNQX, Sigma-Aldrich Japan)—were used. APB is an agonist of the type 6 metabotropic glutamate receptor, and it blocks signal transmission between the photoreceptors and depolarizing or ON-bipolar cells.[19] CNQX is an antagonist of the α-amino-3-hydroxy-5-methyl-4-isoxazolepropionic acid/kainic acid (AMPA/KA) class of ionotropic glutamate receptors and is known to block the light responses of the hyperpolarizing or OFF-bipolar cells, horizontal cells, and all third-order retinal neurons.[20] Thus, the combination of APB and CNQX is expected to isolate the photoreceptor responses. We could not use PDA,[21] another type of antagonist of the AMPA/KA class of ionotropic glutamate receptors, because PDA was not commercially available. Intravitreal concentrations were 2 to 4 mM for APB and 0.2 to 0.4 mM for CNQX, assuming that the vitreous volume of the NZW rabbit is 1.5 mL.[22] The drugs were dissolved in 0.05 mL saline.

Recordings were begun approximately 60 to 90 minutes after the drug injections, and studies were completed within 3 hours. Although the drug effects were reversible, we only used the rabbits that had not been used for any previous experiments.

Measurement of a-Waves

To determine the photoreceptor and post-photoreceptoral contributions to the a-wave of the photopic ERGs quantitatively, we measured the amplitude of the a-wave before and after drug administration. Before drug administration, the a-wave amplitude was measured from the baseline to the first negative trough; after it, the a-wave amplitude was measured from the baseline to the potential at the time of the a-wave peak before the drugs (Fig. 1A). Then the percentage cone photoreceptor contribution was calculated by the expression (a-wave amplitude after APB and CNQX)/(a-wave amplitude before drugs) × 100. This method has been used to determine the degree of cone photoreceptor contribution to the a-wave.[3]

Statistical Analysis

Because the data were normally distributed, unpaired Student's *t*-tests were used to determine whether the amplitude of the a-wave of WT rabbits was significantly different from that of Tg rabbits. Differences were considered to be significant when $P < 0.05$.

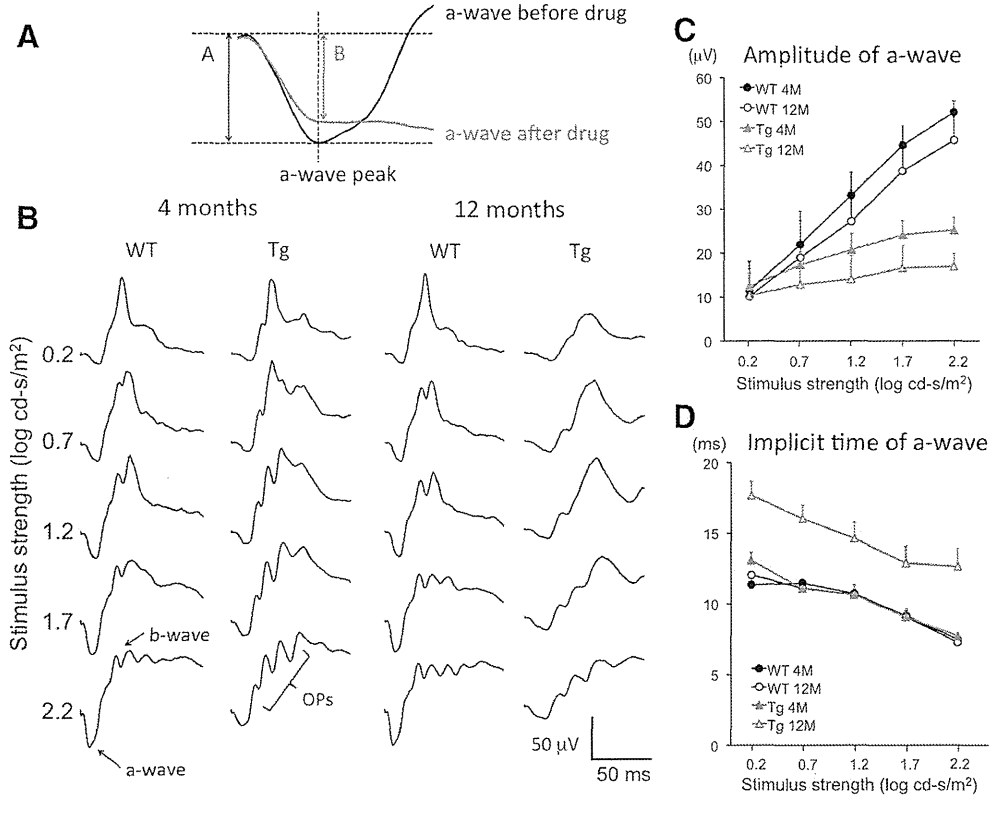

Figure 1. Photopic ERGs of WT and rhodopsin P347L Tg rabbits. (**A**) Method of measuring a-wave amplitude. The a-wave amplitude before drug administration was measured from the baseline to the first negative trough. (**B**) The a-wave amplitude after drug administration was measured from the baseline to the negative value at the time of the a-wave peak before drug administration. Representative photopic ERGs recorded from WT and Tg rabbits at 4 and 12 months of age. ERG waveforms to five different stimulus strengths of 0.2 to 2.2 log cd-s/m^2 are shown. (**C**) Plots of the a-wave amplitude to five different stimulus strengths. Results of WT and Tg rabbits at 4 and 12 months of age are shown. Bars indicate the SE of the means of five animals. (**D**) Plots of the a-wave implicit times to five different stimulus strengths. Results of WT and Tg rabbits at 4 and 12 months of age are shown. Bars indicate the SE of the means of five animals.

RESULTS

Photopic ERGs of WT and Tg Rabbits

Representative photopic ERGs recorded from WT and Tg rabbits at 4 and 12 months of age are shown in Figure 1B. The ERG waveforms elicited by five different stimulus strengths from 0.2 to 2.2 log cd-s/m^2 are shown. We found that all the ERG components of Tg rabbits decreased progressively with increasing age; the a-wave was more affected than the b-wave. These general ERG findings agree with the results reported in our earlier publications.[13,15]

The amplitudes of the a-waves of the photopic ERGs of Tg rabbits were significantly smaller than those of WT rabbits at 4 months of age and even smaller at 12 months of age (Figs. 1B, 1C). The implicit times of the photopic ERG a-wave were not significantly different between the Tg and WT rabbits when they were 4 months of age, but the Tg rabbits had severely delayed implicit times when they were 12 months of age (Fig. 1D).

Effect of APB or CNQX Alone on Photopic ERG a-Wave

To confirm that the a-waves of the photopic ERG in rabbits originated from the same neurons as macaque monkeys, we examined the effect of APB or CNQX alone on the a-wave of the photopic ERGs in WT and Tg rabbits when they were 4 months of age (Fig. 2). We found that intravitreal injection of APB did not alter the leading edge of the photopic a-wave, and the maximal a-wave amplitudes were nearly the same before and after the APB injection for both WT and Tg rabbits (Fig. 2, upper trace). In contrast, an intravitreal injection of CNQX significantly changed the leading edge of the a-wave, and the maximal a-wave amplitude was significantly reduced in both types of rabbits (Fig. 2, lower trace). These results were comparable to the results in primates[3–6] and support the belief that the photopic ERG a-wave receives significant contributions from post-photoreceptoral neurons, including OFF-bipolar cells and horizontal cells in both WT and Tg rabbits.

Amplitude Changes of Photopic ERG a-Wave after Pharmacologic Drug Administration

We next examined the contribution of the cone photoreceptors to the photopic ERG a-wave at the time of the a-wave peak. The black lines in Figure 3 show the photopic ERG a-waves before drugs, and the color lines (blue, WT; red, Tg) show the ERG waveforms after intravitreal injection of a solution of combined APB and CNQX (i.e., the cone photoreceptor response). The vertical dotted lines show the timing of the a-wave peaks before drug administration. As reported in primates,[3–6] the a-wave amplitude is greatly reduced after blocking all post-photoreceptoral neurons by glutamate analogs.

Mean amplitudes of the a-wave before and after drug administration at the time of the a-wave peak (Fig. 1A), are plotted in Figure 4. The a-wave amplitude decreased after injection of both APB and CNQX for all stimulus strengths in both WT and Tg rabbits.

Relative Contributions of Cone Photoreceptors to Photopic a-Wave

We next compared the relative contributions of the cone photoreceptors with the photopic ERG a-wave for the two types of rabbits. For this, we calculated the percentage contribution of the cone photoreceptors; that is, we divided the a-wave amplitude after APB+CNQX by the a-wave amplitude before drug administration (Fig. 5). We found that the percentage contribution of the cone photoreceptors became greater with increasing stimulus strengths in both WT and Tg rabbits, which is consistent with the findings in normal macaque monkeys.[3] The percentage contribution of the cone photoreceptors ranged from 32% to 51% in Tg rabbits, which was significantly smaller than that in WT rabbits at 54% to 75%, at 4 months of age ($P < 0.01$; Fig. 5, left).

We also calculated these values when the animals were 12 months of age. The percentage contribution of the cone photoreceptors ranged from 11% to 48% in Tg rabbits, which was also significantly smaller than that in WT rabbits at 41% to 70% ($P < 0.05$; Fig. 5, right). The percentage contribution of cone

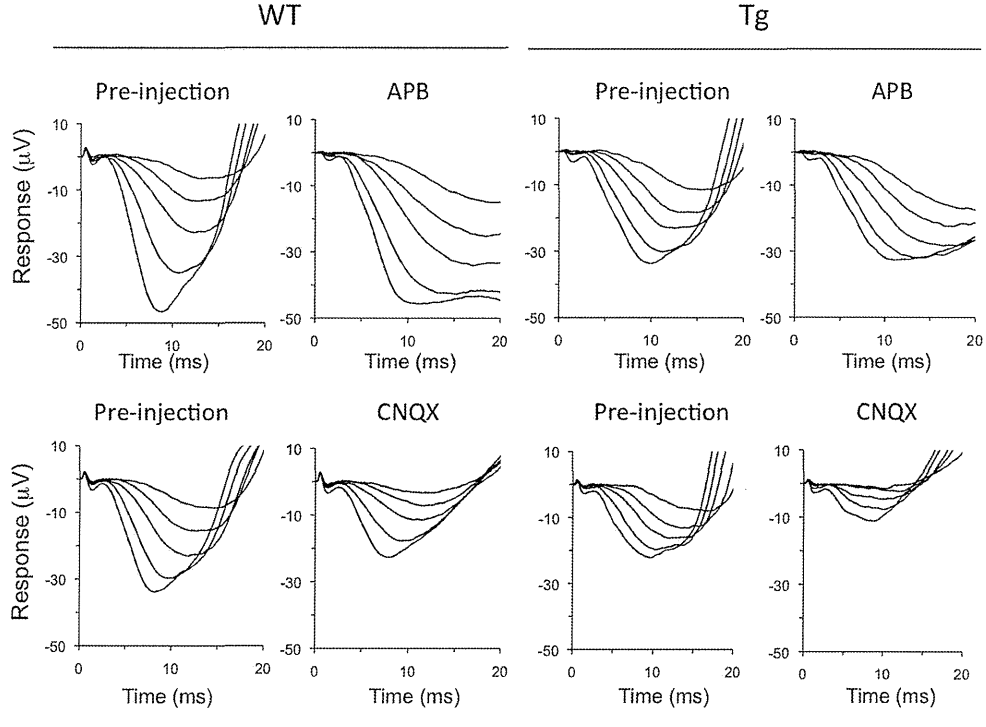

FIGURE 2. Representative waveforms of photopic ERG a-wave before and after APB or CNQX alone in WT and Tg rabbits of 4 months of age. ERG waveforms to five different stimulus strengths of 0.2 to 2.2 log cd-s/m^2 are superimposed.

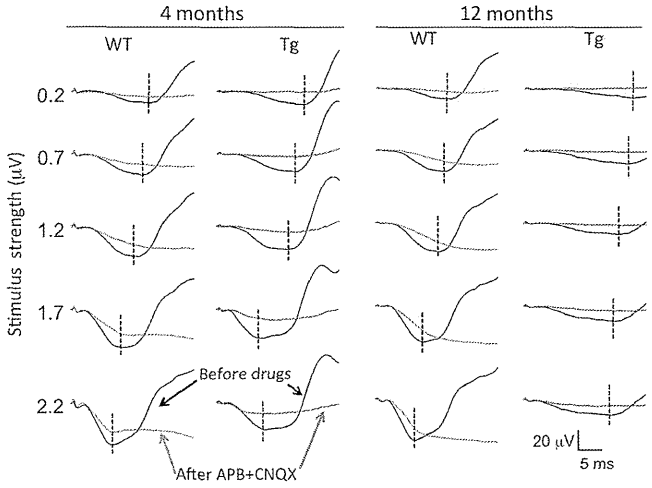

FIGURE 3. Representative waveforms of photopic ERG a-wave before (*black*) and after (*blue* and *red*) intravitreal injection of combination of APB and CNQX in WT and Tg rabbits at 4 and 12 months of age. *Vertical dotted lines*: timing of the a-wave peaks before drug administration.

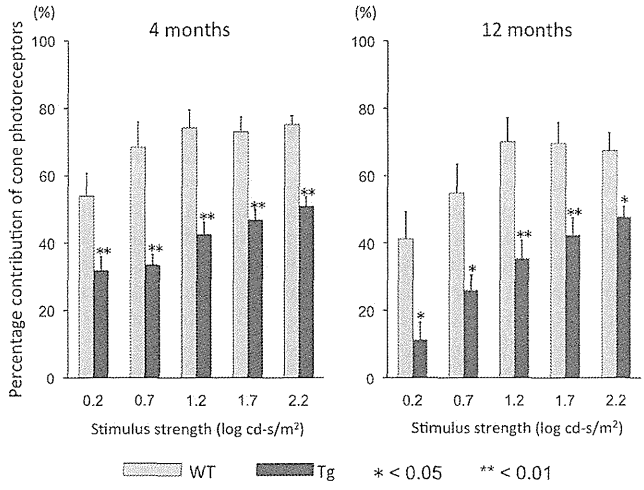

FIGURE 5. Plots of the percentage contribution of cone photoreceptors to the photopic ERG a-wave in WT (*blue*) and Tg (*red*) rabbits at 4 and 12 months of age. Bars indicate the SE of the means of five animals. $^{*}P < 0.05$; $^{**}P < 0.01$.

photoreceptors to the photopic a-wave in 12-month-old Tg rabbits was <50% for all stimulus strengths.

Comparison of Postreceptoral Components

The smaller contributions of cone photoreceptors to the photopic a-waves in Tg rabbits can be explained simply by a decrease in cone photoreceptor responses caused by the photoreceptor degenerations, which can be clearly seen in Figure 4. However, it can also be caused by an increase in neural activities of the post-photoreceptoral neurons. To investigate whether the latter explanation was the cause, we calculated the amplitudes of post-photoreceptoral components at the time of the a-wave peak by subtracting the post-APB+CNQX waveform from the predrug waveform. Results are plotted in Figure 6.

Although the maximal amplitudes of the post-photoreceptoral components were not significantly different in WT and Tg rabbits, the intensity amplitude function for the two types of rabbits were different when they were 4 months of age (Fig. 6, left). The amplitude of the post-photoreceptoral component was nearly saturated at lower stimulus strengths of 0.7 to 1.2 log cd-s/m^2 in Tg rabbits. In contrast, this value increased gradually and reached maximum amplitude at the highest stimulus strength of 2.2 log cd-s/m^2 in WT rabbits. The amplitudes of the post-photoreceptoral components in Tg rabbits were significantly larger than those in WT rabbits at lower stimulus strengths of 0.2 and 0.7 log cd-s/m^2 ($P < 0.05$).

A similar tendency of the stimulus strength-amplitude functions of WT and Tg rabbits was also seen when they were 12 months of age, but the overall amplitudes of post-photoreceptoral components of Tg rabbits were greatly reduced, probably because of advanced retinal degeneration. These results indicated that the smaller contribution of cone photoreceptors to the photopic a-wave in young Tg rabbits occurred partially because of the enhanced post-photoreceptoral responses at lower stimulus strengths.

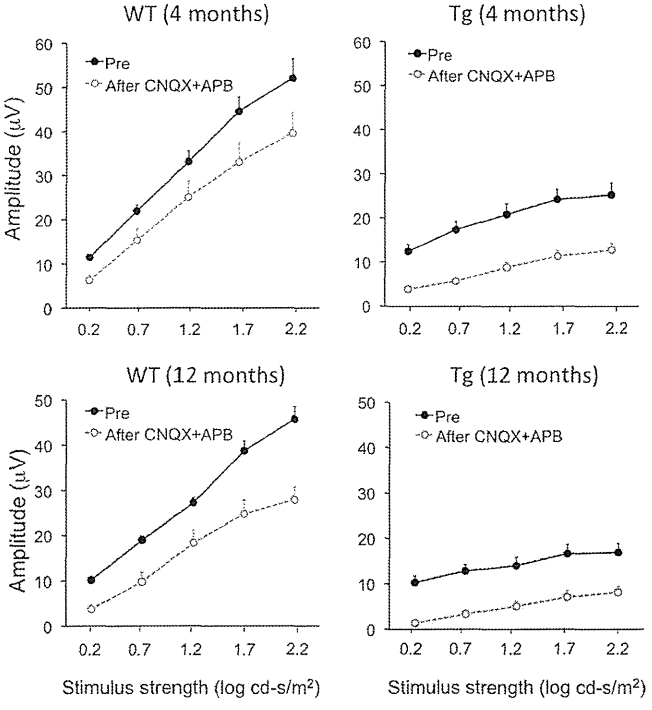

FIGURE 4. Plots of the a-wave amplitude before (*black*) and after (*blue* and *red*) intravitreal injection of combination of APB and CNQX in WT (*left*) and Tg (*right*) rabbits at 4 and 12 months of age. Bars indicate the SE of the means of five animals.

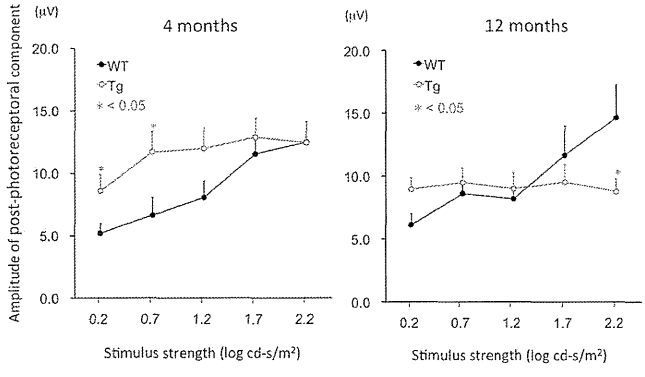

FIGURE 6. Plots of the amplitude of post-photoreceptoral component in the photopic ERG a-wave in WT (*black*) and Tg (*red*) rabbits at 4 and 12 months of age. Bars indicate the SE of the means of five animals. $^{*}P < 0.05$.

Discussion

It is unknown whether the contributions of photoreceptors and post-photoreceptoral neurons are altered in retinas with progressive photoreceptor degeneration. Our present results clearly demonstrated that the percentage contribution of the cone photoreceptors to the photopic a-wave was significantly lower in rhodopsin P347L Tg rabbits than in WT rabbits over a 2 log unit range of stimulus strengths at both 4 and 12 months of age. We found that especially in the retina of 12-month-old Tg rabbits, the percentage contribution of cone photoreceptor to the photopic ERG a-wave was less than half, irrespective of the stimulus strength (Fig. 5, right).

Our results showed that the effects of stimulus strength on the cone photoreceptors and post-photoreceptoral contributions to the photopic a-wave of normal retinas were similar to those in primates reported by Bush and Sieving.[3] They measured the degree of cone photoreceptor and post-photoreceptoral contribution to the photopic a-wave at the time of the a-wave peak in normal macaque monkeys before and after APB and PDA. They did not report the exact percentage values, but they showed[3] that it was relatively low at 55% at the lowest stimulus strengths and that it gradually increased to a maximum of 92% at the highest stimulus strength. They interpreted these findings that the post-photoreceptoral contribution to the photopic a-wave was primarily responsible for the initial 1 to 1.5 log units of strength, whereas cone photoreceptor contribution progressively dominated the photopic a-wave at higher stimulus strengths. We also observed a similar pattern in our WT rabbits (Fig. 5), but the percentage contribution of cone photoreceptor at the highest stimulus strength was higher in macaque (92%) than in our WT rabbits (75%). This difference might have been due to the difference in the type of stimulus (200-ms long-flash stimuli in their study vs. xenon brief-flash stimuli in our study) or difference in species.

We found that the percentage contribution of cone photoreceptors to the photopic a-wave in Tg rabbits was significantly lower than in WT rabbits (Fig. 5). These results are reasonable because the cone photoreceptor is gradually attenuated whereas the middle and inner retinas are still well preserved in Tg rabbits.[13,15] Additional analyses demonstrated that the smaller percentage contribution of cone photoreceptors in young Tg rabbits can be explained, in part, by the enhancement of the amplitudes of the post-photoreceptoral component, especially at lower stimulus strengths (Fig. 6, left). Such enhanced amplitudes of the post-photoreceptoral component in Tg rabbits were no longer present at 12 months in Tg rabbits, probably because of advanced retinal degeneration.

We do not know the exact mechanism for the enhanced amplitudes of the post-photoreceptoral components elicited by weaker stimulus intensities in young Tg rabbits. This enhanced post-photoreceptoral response may be due to secondary functional changes in the OFF-bipolar/horizontal cells or their synapses after progressive photoreceptor degenerations.

Using computational molecular phenotyping, we have recently shown that during the course of rod photoreceptor degeneration, rod ON-bipolar cells switch their phenotype by expressing ionotropic glutamate receptors (iGluRs).[17] We also found that the rod bipolar cells effectively lose rod contacts and make ectopic cone contacts and express iGluRs.[17] This secondary retinal remodeling may contribute to the enhanced post-photoreceptoral responses in our Tg rabbits. Similarly, detailed ERG studies in rhodopsin P347L Tg pigs and rabbits have demonstrated that the electrical activities of the cone ON-pathway were also enhanced at a relatively early stage of retinal degeneration.[18,23] In addition, an increase in the ERG responses from the inner retina (e.g., scotopic threshold response) was also reported in the retina of the aged Royal College of Surgeons rat, a rodent model of retinal degeneration.[24,25]

Taken together, inherited retinal diseases associated with progressive photoreceptor degeneration may lead to different types of functional changes in the post-photoreceptoral retinal circuits, including the ON- and OFF pathways, during a relatively early stage of retinal degeneration.

We believe our results have important clinical implications. The a-wave of the photopic ERG is believed to be shaped primarily by electrical activities of cone photoreceptors in patients. However, the results of this study suggest that the cone photoreceptor function may be overestimated when the amplitude of the cone ERG a-wave is used as an indicator of residual cone photoreceptor functions in patients with progressive photoreceptor degeneration such as RP. Thus, when the standard stimulus strength (3.0 cd-s/m^2 = 0.48 log cd-s/m^2) recommended by the International Society of Clinical Electrophysiology of Vision[1] was used, contributions of the cone photoreceptors to the photopic a-wave was only 34% at the time of the a-wave peak, and the other 66% originated from post-photoreceptoral neurons (Fig. 5, left). Our results suggest that the lower contribution of the cones to the a-waves of the photopic ERGs must be considered in patients with RP.

There are limitations to this study. One was that we assessed the contribution of photoreceptors and post-photoreceptoral components only at the time of the a-wave peak before the drugs. However, the peak time of the a-wave depends on not only the stimulus strength but also on the presence of retinal degeneration (Fig. 1D). In addition, the a-wave can be truncated by the b-wave. To overcome this, we measured the a-wave amplitude at specific times before the b-wave intrusion (10.5 ms for 0.2 log cd-s/m^2, 9.5 ms for 0.7 log cd-s/m^2, 8.5 ms for 1.2 log cd-s/m^2, 7.5 ms for 1.7 log cd-s/m^2, and 6.5 ms for 2.2 log cd-s/m^2), and calculated the percentage cone photoreceptor contribution when the animals were 4 months of age. We found that the cone photoreceptor contribution still tended to be smaller in Tg rabbits than in WT rabbits, and the differences were significant at the two lower stimulus strengths ($P < 0.01$, Supplementary Fig. S1A, http://www.iovs.org/lookup/suppl/doi:10.1167/iovs.11-9006/-/DCSupplemental). We also measured the a-wave amplitude at a single constant time of 7 ms and calculated the percentage cone photoreceptor contribution. Again, the cone photoreceptor contribution tended to be smaller in Tg rabbits than in WT rabbits, but the difference was significant only at the highest stimulus strength (Supplementary Fig. S1B, http://www.iovs.org/lookup/suppl/doi:10.1167/iovs.11-9006/-/DCSupplemental).

In summary, our results indicate that the relative contribution of cone photoreceptors to the photopic ERG a-wave is smaller in retinas with inherited photoreceptor degeneration. These results suggest that care must be taken in interpreting the a-wave amplitudes of photopic ERGs in patients with progressive photoreceptor degeneration.

Acknowledgments

The authors thank Duco I. Hamasaki for editing the manuscript and Michael Bach for helpful discussions.

References

1. Marmor MF, Fulton AB, Holder GE, et al. ISCEV Standard for full-field clinical electroretinography (2008 update). *Doc Ophthalmol.* 2009;118:69–77.
2. Frishman LJ. Origins of the electroretinogram. In: Heckenlively JR, Arden GB, eds. *Principles and Practice of Clinical Electrophysiology of Vision.* 2nd ed. London: MIT Press; 2006:139–183.
3. Bush RA, Sieving PA. A proximal retinal component in the primate photopic ERG a-wave. *Invest Ophthalmol Vis Sci.* 1994;35:635–645.

4. Sieving PA, Murayama K, Naarendorp F. Push-pull model of the primate photopic electroretinogram: a role for hyperpolarizing neurons in shaping the b-wave. *Vis Neurosci.* 1994;11:519–532.
5. Jamison JA, Bush RA, Lei B, Sieving PA. Characterization of the rod photoresponse isolated from the dark-adapted primate ERG. *Vis Neurosci.* 2001;18:445–455.
6. Robson JG, Saszik SM, Ahmed J, Frishman LJ. Rod and cone contributions to the a-wave of the electroretinogram of the macaque. *J Physiol.* 2003;547:509–530.
7. Friedburg C, Allen CP, Mason PJ, Lamb TD. Contribution of cone photoreceptors and post-receptoral mechanisms to the human photopic electroretinogram. *J Physiol.* 2004;556:819–834.
8. Sharma S, Ball SL, Peachey NS. Pharmacological studies of the mouse cone electroretinogram. *Vis Neurosci.* 2005;22:631–636.
9. Bui BV, Fortune B. Origin of electroretinogram amplitude growth during light adaptation in pigmented rats. *Vis Neurosci.* 2006;23:155–67.
10. Koyasu T, Kondo M, Miyata K, et al. Photopic electroretinograms of mGluR6-deficient mice. *Curr Eye Res.* 2008;33:91–99.
11. Miura G, Wang MH, Ivers KM, Frishman LJ. Retinal pathway origins of the pattern ERG of the mouse. *Exp Eye Res.* 2009;89:49–62.
12. Shirato S, Maeda H, Miura G, Frishman LJ. Postreceptoral contributions to the light-adapted ERG of mice lacking b-waves. *Exp Eye Res.* 2008;86:914–928.
13. Kondo M, Sakai T, Komeima K, et al. Generation of a transgenic rabbit model of retinal degeneration. *Invest Ophthalmol Vis Sci.* 2009;50:1371–1377.
14. Dryja TP, Hahn LB, Cowley GS, et al. Mutation spectrum of the rhodopsin gene among patients with autosomal dominant retinitis pigmentosa. *Proc Natl Acad Sci U S A.* 1991;88:9370–9374.
15. Sakai T, Kondo M, Ueno S, et al. Supernormal ERG oscillatory potentials in transgenic rabbit with rhodopsin P347L mutation and retinal degeneration. *Invest Ophthalmol Vis Sci.* 2009;50:4402–449.
16. Yokoyama D, Machida S, Kondo M, et al. Pharmacological dissection of multifocal electroretinograms of rabbits with Pro347Leu rhodopsin mutation. *Jpn J Ophthalmol.* 2010;54:458–466.
17. Jones BW, Kondo M, Terasaki H, et al. Retinal remodeling in the Tg P347L rabbit, a large-eye model of retinal degeneration. *J Comp Neurol.* 2011;519:2713–2733.
18. Nishimura T, Machida S, Kondo M, et al. Enhancement of ON-bipolar cell responses of cone electroretinograms in rabbits with Pro347Leu rhodopsin mutation. *Invest Ophthalmol Vis Sci.* 2011;52:7610–7617.
19. Slaughter MM, Miller RF. 2-Amino-4-phosphonobutyric acid: a new pharmacological tool for retina research. *Science.* 1981;211:182–185.
20. Honoré T, Davies SN, Drejer J, et al. Quinoxalinediones: potent competitive non-NMDA glutamate receptor antagonists. *Science.* 1988;241:701–703.
21. Slaughter MM, Miller RF. An excitatory amino acid antagonist blocks cone input to sign-conserving second-order retinal neurons. *Science.* 1983;219:1230–1232.
22. Leeds JM, Henry SP, Truong L, et al. Pharmacokinetics of a potential human cytomegalovirus therapeutic, a phosphorothioate oligonucleotide, after intravitreal injection in the rabbit. *Drug Metab Dispos.* 1997;25:921–926.
23. Banin E, Cideciyan AV, Alemán TS, et al. Retinal rod photoreceptor-specific gene mutation perturbs cone pathway development. *Neuron.* 1999;23:549–557.
24. Bush RA, Hawks KW, Sieving PA. Preservation of inner retinal responses in the aged Royal College of Surgeons rat: evidence against glutamate excitotoxicity in photoreceptor degeneration. *Invest Ophthalmol Vis Sci.* 1995;36:2054–2062.
25. Machida S, Raz-Prag D, Fariss RN, et al. Photopic ERG negative response from amacrine cell signaling in RCS rat retinal degeneration. *Invest Ophthalmol Vis Sci.* 2008;49:442–452.

OPEN ACCESS Freely available online

PLoS one

Identification of Autoantibodies against TRPM1 in Patients with Paraneoplastic Retinopathy Associated with ON Bipolar Cell Dysfunction

Mineo Kondo[1*☯], Rikako Sanuki[2,3☯], Shinji Ueno[1], Yuji Nishizawa[4], Naozumi Hashimoto[5], Hiroshi Ohguro[6], Shuichi Yamamoto[7], Shigeki Machida[8], Hiroko Terasaki[1], Grazyna Adamus[9], Takahisa Furukawa[2,3*]

1 Department of Ophthalmology, Nagoya University Graduate School of Medicine, Nagoya, Aichi, Japan, **2** Department of Developmental Biology, Osaka Bioscience Institute, Suita, Osaka, Japan, **3** JST, CREST, Suita, Osaka, Japan, **4** Department of Biomedical Sciences, Chubu University, Kasugai, Aichi, Japan, **5** Department of Respiratory Medicine, Nagoya University Graduate School of Medicine, Nagoya, Aichi, Japan, **6** Department of Ophthalmology, Sapporo Medical University School of Medicine, Sapporo, Hokkaido, Japan, **7** Department of Ophthalmology and Visual Science, Chiba University Graduate School of Medicine, Chiba, Chiba, Japan, **8** Department of Ophthalmology, Iwate Medical University School of Medicine, Morioka, Iwate, Japan, **9** Department of Ophthalmology, Oregon Health and Science University, Portland, Oregon, United States of America

Abstract

Background: Paraneoplastic retinopathy (PR), including cancer-associated retinopathy (CAR) and melanoma-associated retinopathy (MAR), is a progressive retinal disease caused by antibodies generated against neoplasms not associated with the eye. While several autoantibodies against retinal antigens have been identified, there has been no known autoantibody reacting specifically against bipolar cell antigens in the sera of patients with PR. We previously reported that the transient receptor potential cation channel, subfamily M, member 1 (TRPM1) is specifically expressed in retinal ON bipolar cells and functions as a component of ON bipolar cell transduction channels. In addition, this and other groups have reported that human TRPM1 mutations are associated with the complete form of congenital stationary night blindness. The purpose of the current study is to investigate whether there are autoantibodies against TRPM1 in the sera of PR patients exhibiting ON bipolar cell dysfunction.

Methodology/Principal Findings: We performed Western blot analysis to identify an autoantibody against TRPM1 in the serum of a patient with lung CAR. The electroretinograms of this patient showed a severely reduced ON response with normal OFF response, indicating that the defect is in the signal transmission between photoreceptors and ON bipolar cells. We also investigated the sera of 26 patients with MAR for autoantibodies against TRPM1 because MAR patients are known to exhibit retinal ON bipolar cell dysfunction. Two of the patients were found to have autoantibodies against TRPM1 in their sera.

Conclusion/Significance: Our study reveals TRPM1 to be one of the autoantigens targeted by autoantibodies in at least some patients with CAR or MAR associated with retinal ON bipolar cell dysfunction.

Citation: Kondo M, Sanuki R, Ueno S, Nishizawa Y, Hashimoto N, et al. (2011) Identification of Autoantibodies against TRPM1 in Patients with Paraneoplastic Retinopathy Associated with ON Bipolar Cell Dysfunction. PLoS ONE 6(5): e19911. doi:10.1371/journal.pone.0019911

Editor: Steven Barnes, Dalhousie University, Canada

Received February 10, 2011; **Accepted** April 6, 2011; **Published** May 17, 2011

Funding: This work was supported by CREST from the Japan Science and Technology Agency (http://www.jst.go.jp/), and a Grant-in-Aid for Scientific Research (B)(C) (#20390448, #20390087, #20592075, #20791678) from the Ministry of Education, Culture, Sports, Science and Technology (http://www.jsps.go.jp/), the Takeda Science Foundation (http://www.takeda-sci.or.jp/), The Uehara Memorial Foundation (http://www.ueharazaidan.com/), the Naito Foundation (http://www.naito-f.or.jp/), the Novartis Foundation (#20-10, http://novartisfound.or.jp/), Mochida Memorial Foundation for Medical and Pharmaceutical Research (http://www.mochida.co.jp/zaidan/), the Senri Life Science Foundation (#S-2144, http://www.senri-life.or.jp/), the Kato Memorial Bioscience Foundation (http://www.katokinen.or.jp/) and the Japan National Society for the Prevention of Blindness (http://www.nichigan.or.jp/link/situmei.jsp). A grant from the National Institute of Health (E13053), was awarded to GA. The funders had no role in study design, data collection and analysis, decision to publish, or preparation of the manuscript.

Competing Interests: The authors have declared that no competing interests exist.

* E-mail: furukawa@obi.or.jp (TF); kondomi@med.nagoya-u.ac.jp (MK)

☯ These authors contributed equally to this work.

Introduction

Paraneoplastic retinopathy (PR) is a progressive retinal disorder caused by an autoimmune mechanism and is associated with the presence of anti-retinal antibodies in the serum generated against neoplasms not associated with the eye [1–4]. The retinopathy can develop either before or after the diagnosis of a neoplasm. Patients with PR can have night blindness, photopsia, ring scotoma, attenuated retinal arteriole, and abnormal electroretinograms (ERGs). The diagnosis of PR is usually made by the identification of neoplasms and anti-retinal autoantibodies in the sera.

PR includes two subgroups: cancer-associated retinopathy (CAR) [5,6] and melanoma-associated retinopathy (MAR) [7–10]. Although CAR and MAR share similar clinical symptoms, the ERG findings

are very different. Both a- and b-waves are severely attenuated in CAR, indicating extensive photoreceptor dysfunction, whereas only the b-wave is severely reduced while the a-wave is normal in MAR, suggesting bipolar cell dysfunction [8,9]. However, it was recently reported that cancers other than melanoma can cause bipolar cell dysfunction [11,12]. Several autoantibodies against retinal antigens have been identified, but a specific antigen associated with bipolar cells has not been identified in patients with CAR and MAR [1–10].

In the current study, we identified autoantibodies against the transient receptor potential cation channel, subfamily M, member 1 (TRPM1) [13–15] in the serum of one patient with lung cancer. The ERG findings in this patient indicated a selective ON-bipolar cell dysfunction. We also investigated the sera of 26 MAR patients and found that two contained autoantibodies against TRPM1. Our results suggest that TRPM1 is one of the retinal autoantigens in at least some patients with CAR or MAR and may cause retinal ON bipolar cell dysfunction.

Results

Case report of CAR associated with ON bipolar cell dysfunction

A 69-year-old man visited the Nagoya University Hospital with complaints of blurred vision, photopsia and night blindness in both eyes of three months duration. At this point he was not diagnosed as suffering from any eye disease or systemic disease, including a malignant tumor, and his family history revealed no other members suffering from any eye diseases. On initial examination, his best-corrected visual acuity was 0.9 in the right eye and 0.6 in the left eye. Humphrey static perimetry revealed a severe decrease in sensitivity within the central 30 degrees of the visual field in both eyes (Fig. 1A). Dark-adaptometry of this patient showed a loss of the rod branch. The cone threshold was within normal range. Ophthalmoscopy showed a nearly normal fundus appearance except for slight hypopigmentation at the macula of the left eye, which may be due to age-related changes in the retinal pigment epithelium (Fig. 1B), but fluorescein angiography demonstrated periphlebitis of the retinal vessels (arrows, Fig. 1C). Spectral-domain optical coherence tomography (SD-OCT) showed that the morphology of the retina was normal in both eyes (Fig. 1D).

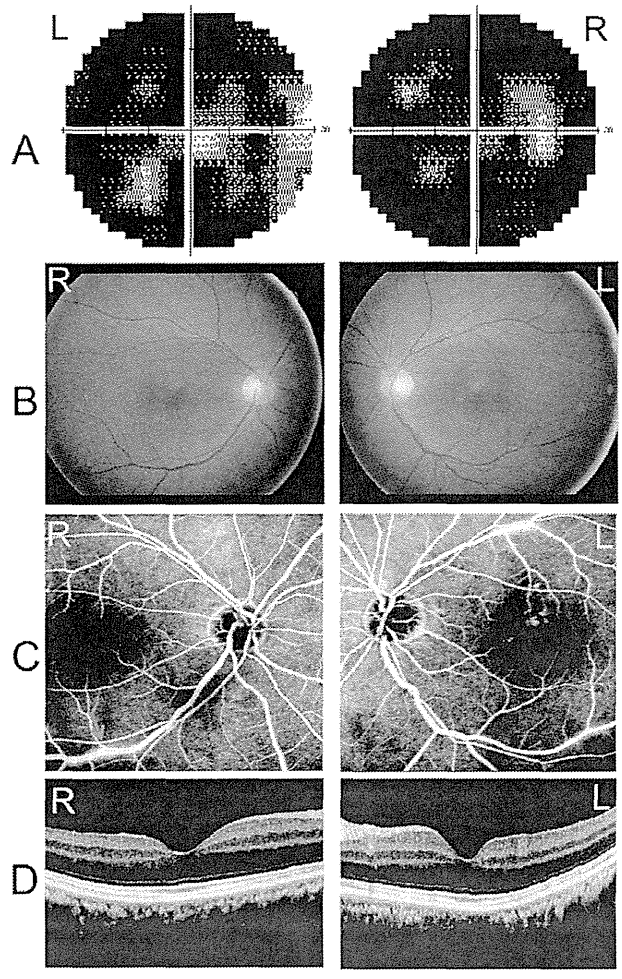

Figure 1. Ophthalmological findings from a patient with paraneoplastic retinopathy (PR) associated with lung cancer. (A) Threshold of static visual field (Humphrey, 30-2 program) plotted on a gray scale showing severely decreased sensitivities within the central 30 degrees of the visual field. (B) Fundus photographs of the patient showing a nearly normal fundus. (C) Fluorescein angiograms showing periphlebitis of the retinal vessels (arrows). (D) Spectral-domain optical coherence tomographic (SD-OCT) image of a 9 mm horizontal scan of the retina of our patient. The retinal structure in each retinal layer is normal.
doi:10.1371/journal.pone.0019911.g001

Electrophysiological examinations

Recordings of the full-field ERGs from this patient showed that the rod responses were undetectable (Fig. 2). The rod- and cone-mixed maximal response was a negative-type with an a-wave of normal amplitude and a b-wave that was smaller than the a-wave. The a-wave of the cone response had a wide trough, and the b-wave was reduced by 40%. The amplitude of the 30-Hz flicker ERG was reduced by 50%. The photopic long-flash ERG showed severely reduced ON response and normal OFF response. These ERG findings indicated that there was a defect in the signal transmission from photoreceptors to ON bipolar cells both in both rod and cone pathways.

Based on these ophthalmological and electrophysiological tests, we suspected that this patient might have PR and referred him to an internist. The general physical examination including positron emission tomography and computed tomography revealed two abnormal masses in the right lung. Biopsy of these masses confirmed that the masses were small cell carcinomas of the lung.

Detection of autoantibodies against TRPM1 in the serum of the CAR patient

Based on our ERG examination results, we hypothesized that the serum of this CAR patient may contain autoantibodies against TRPM1. To test this hypothesis, we examined whether or not this CAR patient's serum could recognize human TRPM1 protein by Western blot analysis. We transfected an expression plasmid containing human TRPM1 cDNA with the C-terminal 3xFlag-tag (TRPM1-3xFlag) into HEK293T cells, and carried out a Western blot analysis using whole cell extracts harvested after 48 hrs cell growth. We first confirmed that TRPM1-3xFlag was expressed by cell using Western blot analysis and an anti-Flag antibody. We detected the ~200 kDa TRPM1-3xFlag band in the cell lysates (Fig. 3A).

Next, we performed Western blot analysis on the same lysates using the serum from our CAR patient and a healthy control person. We detected immunostaining of the same size protein, which was confirmed with the anti-Flag antibody, and with CAR serum. The control serum did not present a significant band (Fig. 3B, C). This result showed the presence of autoantibodies against TRPM1 in this CAR patient's serum.

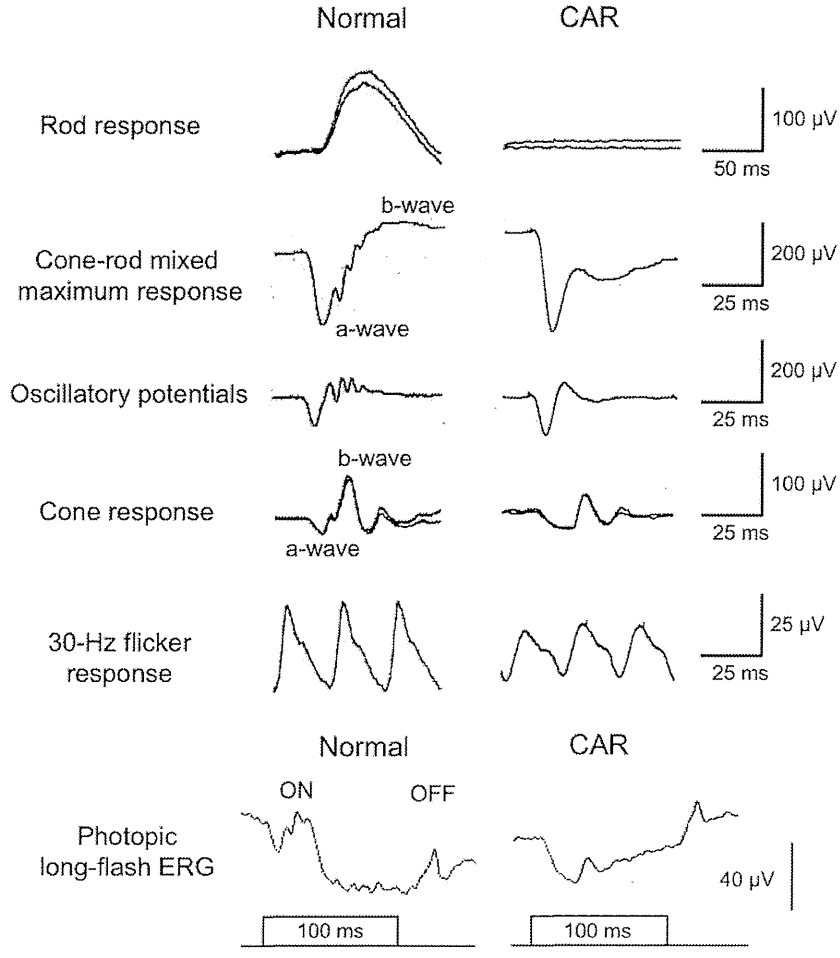

Figure 2. Full-field ERG recordings. The rod response was recorded with a blue light at an intensity of 5.2×10^{-3} cd-s/m^2 after 30 minutes of dark-adaptation. The cone-rod mixed maximum response was elicited by a white flash at an intensity of 44.2 cd-s/m^2. The oscillatory potentials were recorded with a white flash at an intensity of 44.2 cd-s/m^2 using a band-pass filter of 50–1000 Hz. The cone response and a 30 Hz flicker response were elicited by a white stimulus of 4 cd-s/m^2 and 0.9 cd-s/m^2, respectively, on a blue background of 30 cd/m^2. Photopic long-flash ERG responses were also elicited by long-duration flashes of 100 ms using a densely-packed array of white LEDs of 200 cd/m^2 on a white background of 30 cd/m^2.
doi:10.1371/journal.pone.0019911.g002

To examine whether the serum from the CAR patient recognized retinal bipolar cells, we carried out an immunohistochemical analysis on monkey and mouse retinas. We first performed immunohistochemistry on the retina of a 3-year-old rhesus monkey (*Macaca mulata*) and on the retina of a one-month-old C57/B6 mouse using the serum of the CAR patient, however, we did not obtain a significant staining signal above background (data not shown). We then concentrated the serum by IgG purification followed by filter spin column centrifugation and performed immunohistochemistry on the monkey retina using the concentrated serum (Fig. 3D–G). We observed a significant immunolabeling on the INL in the monkey retina (Fig. 3D, F) whereas the normal serum did not give a significant labeling (Fig. 3E, G). The antibodies immuolabeled both the bipolar side and amacrine side of the INL. Since most of the cells residing on the outer side of the INL are ON bipolar cells, at least some of the stained cells are ON bipolar cells. It should be noted some of the staining signals show a spotted pattern in the outer plexiform layer (Fig. 3F) as is observed in TRPM1 or mGluR6 immunostaining on the mouse retina [13], suggesting that the CAR patient serum recognizes the bipolar dendritic tips where some of the TRPM1 protein localizes.

Western blot analysis of the sera from MAR patients

Since the functional defect in the retina of MAR patients is known to be due to abnormal signal transmission between photoreceptors and ON bipolar cells [8,9], we then investigated whether or not autoantibodies to TRPM1 were also present in the sera of MAR patients. We obtained the sera of 26 MAR patients from two hospitals in Japan (Chiba University Hospital and Iwate Medical University Hospital) and Ocular Immunology Laboratory in the USA (Casey Eye Institute). We found that the sera from patients #8 and #23 exhibited a significant immunoreactive band against TRPM1-transfected cell lysates by Western blot analysis (Fig. 4A and B). The control serum showed no significant immune response against the TRPM1-transfected cell lysates (Fig. 3C). These results suggest that the sera from some MAR patients contain autoantibodies against TRPM1. Due to the limited volume of sera from the MAR patients, we could not try immunostaining on the monkey or the mouse retina using the serum from the patients #8 and #23.

MAR patient #8, was a 76-year-old man with a history of skin melanoma. He had ring scotomas and abnormal ERGs indicating that he had MAR. The other patient, MAR #23, was a 57-year-

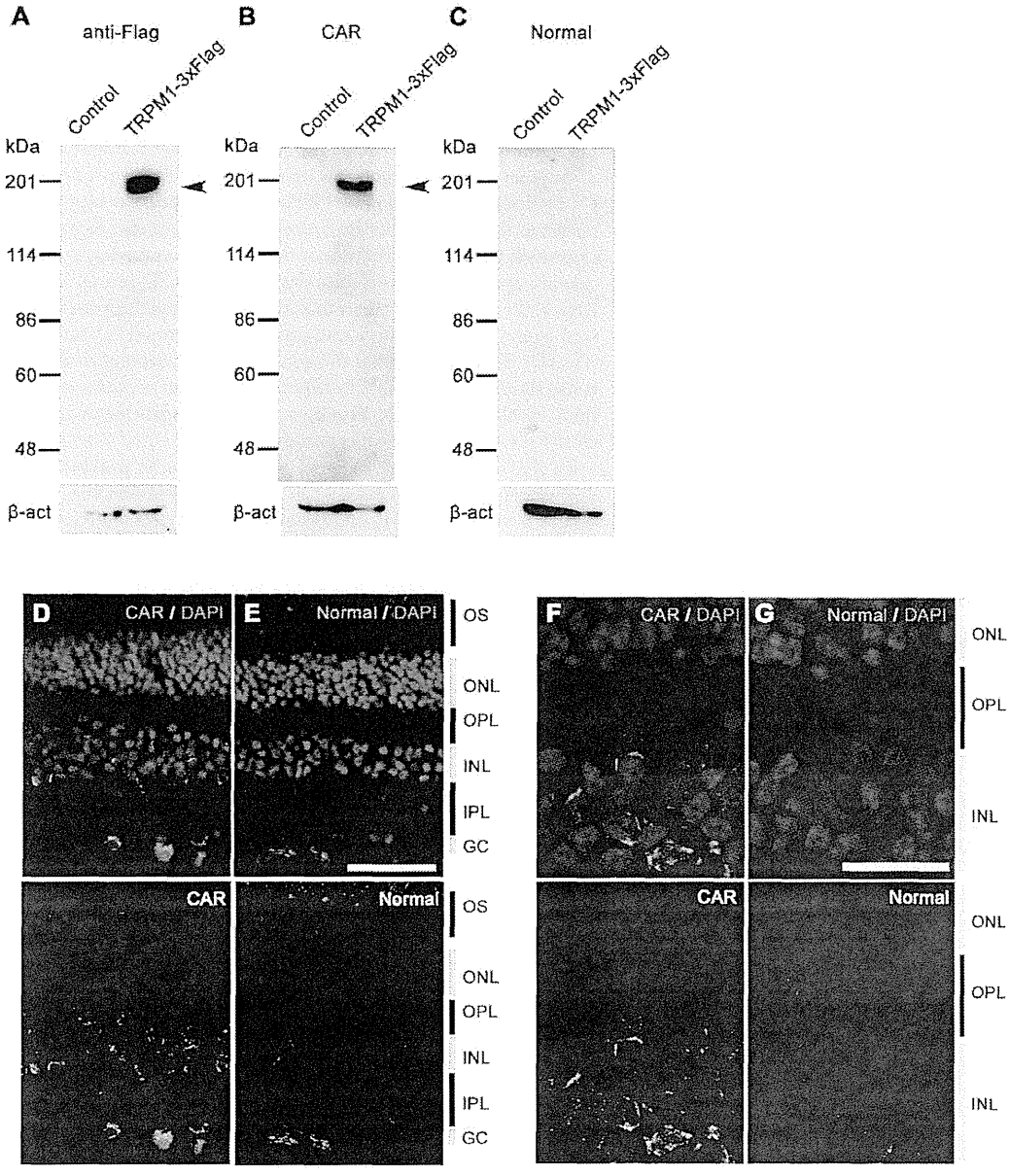

Figure 3. Immunostaining and Western blot analysis of human TRPM1 using serum from the CAR patient. (A–C) Immunoblots of the transfected cell lysates using an antibody against Flag tag (A), serum from CAR patient (B), and control serum (C). Arrowheads indicate the TRPM1-3xFlag protein bands. HEK293T cells were transfected with the pCAGGS or pCAGGS-human TRPM1-3xFlag plasmid, and cells were harvested after 48 hrs. β-actin (β-act) was used for a loading control. (D–G) Confocal images of a three-year-old rhesus monkey retina immunostained with the concentrated serum from the CAR patient (D, F) or the concentrated normal serum (E, G). Cell nuclei are visualized with DAPI. CAR patient serum presented signals on INL cells and the inner part of the OPL (D, F). Scale bar = 50 μm in (E) and 20 μm in (G).
doi:10.1371/journal.pone.0019911.g003

old man with poor night vision, abnormal scotopic ERGs and abnormal color vision. He had a history of skin melanoma and thyroid cancer. There was no other clinical information available on these two patients because these sera were obtained from other institutes several years before without detailed clinical information.

Discussion

PR, including MAR and CAR, presents visual disorders associated with systemic cancer. Antibodies against retinal cells and proteins have been detected in the sera of patients with PR suggesting an autoimmune basis for the etiology of the PR. The autoantibodies identified so far include rhodopsin, retinal transducin alpha and beta, recoverin, S-arrestin, α-enolase, carbonic anhydrase II, and heat shock protein-60 which reside abundantly in photoreceptors [1–10,16]. MAR and CAR can cause bipolar cell dysfunction [7–12]. The results of the ERG [8,9] and immunohistochemistry [7] studies suggested that the main target of MAR are retinal ON bipolar cells in both the rod and cone pathways. However, autoantibodies specifically reacting with a bipolar cell antigen had not been identified in the sera of patients with PR, including those with CAR and MAR. In the current study, we identified autoantibodies against TRPM1, a component of the ON bipolar cell transduction channel negatively regulated by Goα in the mGluR6 signaling pathway [13–15], in the

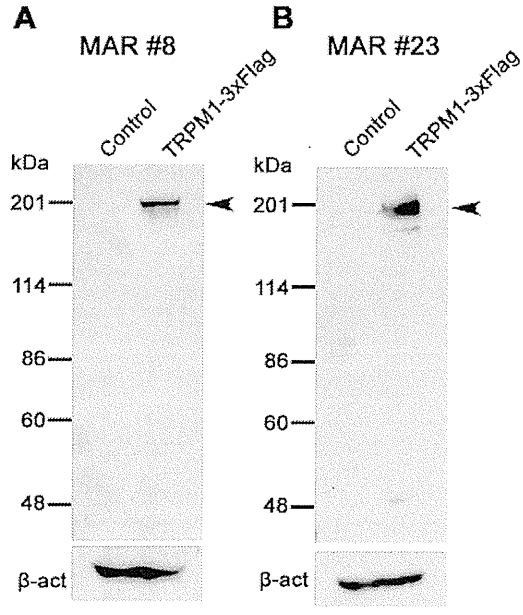

Figure 4. Western blot analysis of human TRPM1 using sera from the MAR patients. (A, B) Immunoblots of the transfected cell lysates using sera from MAR patient #8 (A) and MAR patient #23 (B). HEK293T cells were transfected with pCAGGS or pCAGGS-human TRPM1-3xFlag plasmid, and cells were harvested after 48 hrs. Arrowheads indicate the TRPM1-3xFlag protein bands. β-actin (β-act) was used for a loading control.
doi:10.1371/journal.pone.0019911.g004

sera of one CAR patient and two MAR patients. The CAR patient exhibited a dysfunction of ON bipolar cells, and to our knowledge, this is the first report on an autoantibody against a bipolar cell antigen in the serum of PR patients affecting the ON bipolar cell function.

Previously, we isolated a mouse *TRPM1-L* cDNA corresponding to the human long form of *TRPM1*, and found that the TRPM1-L protein is developmentally localized at the tips of the ON bipolar dendrites co-localizing with mGluR6, but not on OFF bipolar cells [13,14]. The *TRPM1* null mutant mouse completely loses the ON bipolar cell photoresponses to light, indicating that TRPM1 plays a critical role in the synaptic transmission from photoreceptors to ON-bipolar cells [13,15]. In addition, we demonstrated using a CHO cell reconstitution system that TRPM1-L is a nonselective cation channel which is negatively regulated by Goα downstream of the mGluR6 signaling cascade in ON bipolar cells [13]. Recently, four groups including ours independently reported that mutations of human *TRPM1* are associated with the complete-type of congenital stationary night blindness (cCSNB), an inherited human retinal disease [17–20]. cCSNB is a non-progressive retinal disease characterized by congenital night blindness with a moderate decrease in visual acuity and myopia [21-24]. Previous ERG studies have suggested that the defect in cCSNB patients lies in the signal transmission from photoreceptors to ON bipolar cells in both the rod and cone pathways [25–28]. We have identified five different mutations in our three cCSNB patients, and have shown that these mutations lead to either abnormal TRPM1 protein production or mislocalization of the TRPM1 protein in bipolar cell dendrites [17]. These results suggest that TRPM1 plays a critical role in mediating the photoresponses of ON bipolar cells in humans as well. Based on these findings, we hypothesize that the ectopic expression of TRPM1 in tumor cells of some CAR and MAR patients may result in aberrant production of autoantibodies to TRPM1 through B-lymphocytic responses [29–32]. These antibodies may react to the TRPM1 protein in retinal ON bipolar cells resulting in dysfunction of the TRPM1 transduction cation channel downstream of the mGluR6 signaling cascade. However, we could not confirm whether TRPM1 is expressed in the tumor cells of the three PR patients examined in this study [29] because tumor samples were not available.

Another question regarding the disease mechanism underlying PR is whether the binding of TRPM1 autoantibody to bipolar cells results in the cell death or dysfunction of bipolar cells. As far as we examined the retinal structure of the CAR patient using a spectral domain optical coherence tomography (SD-OCT) retinal imaging device, the structure of the retinal bipolar cell layer appeared to be well preserved even three months after the onset of symptoms (Fig.1D). This suggests that the autoantibodies reacting to TRPM1 cause dysfunction of the ON bipolar transduction pathway rather than bipolar cell death. However, further studies are needed to clarify the exact disease mechanism.

In the sera of MAR patients, several types of autoantibodies against retinal proteins have been reported, including the 22 kDa neuronal antigen GNB1, rhodopsin, S-arrestin, and aldolase-A and -C [10,16,33,34]. We initially considered that TRPM1 might be a major MAR target antigen, because TRPM1 is exclusively expressed in retinal ON bipolar cells. However, autoantibodies against TRPM1 were detected in only two out of 26 MAR. patients' sera (7.7%, Fig. 4A, B). We tested whether the sera of one CAR patient and 26 MAR patients recognized human mGluR6, which is specifically expressed in ON bipolar cells, however, none of the sera exhibited a significant band in Western blot analysis (data not shown). Thus, antigens other than TRPM1 or mGluR6 may be involved in the pathogenesis of a large proportion of MAR.

Immunohistochemical analyses using the serum of the CAR patient showed labeling in the inner nuclear layer and outer plexiform layer of the adult rhesus monkey retina (Fig. 3D–G), where the bipolar cell bodies and dendrites reside, respectively. This immunostaining pattern is somewhat similar to our previous immunostaining results on the mouse retina with specific antibody against mouse TRPM1-L, which corresponds to the human TRPM1 long form [13]. Other labeling was also observed in the amacrine cells and ganglion cells. The reason for the immunoreactivity with these cells is uncertain, however, it may be due to the presence of other autoantibodies against amacrine cell and ganglion cell antigens. Lu *et al.* reported the presence of various different autoantibodies in the serum of a single PR patient [10]. If this is the case, it may explain why our CAR patient displayed severely reduced visual sensitivities in the visual field tests (Fig. 1A) unlike cCSNB patients with TRPM1 mutations[17].

It should be noted that we did not confirm whether there are any antoantibodies against TRPM1 in the sera of normal subjects by using a large number of samples. However, this possibility is thought to be low, because Shimazaki *et al.* reported that the molecular weights of the IgGs with observed anti-retinal reactivity in 92 normal sera were smaller than 148 kDa, which is smaller than the TRPM1 molecular weight of ~200 kDa, although relatively high molecular weight reactivity was not intensively investigated [35].

One limitation of the current study is that we could not obtain detailed information on the two MAR patients, MAR #8 and #23, associated with the TRPM1 autoantibody. We confirmed that these two patients had skin melanomas accompanying the visual disturbances, but could not obtain a more detailed clinical history or data on visual acuity, visual field, or ERGs because these sera were sent from different hospitals several years ago. Thus, we do not know whether these two MAR patients really had retinal ON bipolar cell dysfunction. Further prospective studies of the TRPM1 autoantibodies in large numbers of MAR patients are needed.

In conclusion, our study suggests that TRPM1 may be one of the causative antigens responsible for PR associated with ON bipolar cell dysfunction.

Note added in proof

During the course of revision process of this manuscript, Dhingra *et al.* (J. Neurosci. 31, 3962–3967, 2011) independently reported the presence of autoantibodies against TRPM1 in two MAR patients. Our study reports on autoantibodies against TRPM1 in CAR serum in addition to MAR sera.

Materials and Methods

Subjects

The Nagoya University Hospital Ethics Review Board approved this study (approval ID 1131). Of the PR patients that were examined in the Nagoya University Hospital, one PR patient with lung cancer and ON bipolar cell dysfunction was studied in detail. The examinations included routine ophthalmological and electrophysiological tests. In addition, immunohistochemical and Western blot analyses were performed using the serum of this patient. The procedures used conformed to the tenets of the Declaration of Helsinki of the World Medical Association. A written informed consent was obtained from the patient after he was provided with sufficient information on the procedures to be used.

We also obtained sera of 26 patients with MAR from two hospitals in Japan (Chiba University Hospital and Iwate Medical University Hospital) and Ocular Immunology Laboratory in the USA (Casey Eye Institute) for Western blot analysis.

Ophthalmologic examinations

The ophthalmologic examination included best-corrected visual acuity, biomicroscopy, ophthalmoscopy, fundus photography, fluorescein angiography, static perimetry, and spectral-domain optical coherence tomography (SD-OCT). Static visual fields were obtained with the Humphrey 30-2 program (Carl Zeiss, Dublin, USA), and the results are shown in gray scale. SD-OCT was performed with a 9-mm horizontal scan through the midline with 50 averages (Spectralis HRA+OCT; Heidelberg Engineering, Vista, CA).

Electroretinograms (ERG)

Full-field ERGs were elicited with a Ganzfeld dome and recorded with a Burian-Allen bipolar contact lens electrode. The ground electrode was attached to the ipsilateral ear.

After 30 minutes of dark-adaptation, a rod response was elicited with a blue light at an intensity of 5.2×10^{-3} cd-s/m^2. A cone-rod mixed maximum response was elicited by a white flash at an intensity of 44.2 cd-s/m^2. A cone response and a 30 Hz flicker response were elicited by a white stimulus of 4 cd-s/m^2 and 0.9 cd-s/m^2, respectively, on a blue background of 30 cd/m^2. Full-field cone ERGs were also elicited by long-duration flashes of 100 ms using a densely packed array of white LEDs. The array was positioned at the top of the Ganzfeld dome and covered by a diffuser. The stimulus intensity and background illumination measured in the dome was 200 cd/m^2 and 30 cd/m^2, respectively. Responses were amplified by 10K and the band pass was set to 0.3 to 1000 Hz. The data were digitized at 4.3 kHz, and 5 to 20 responses were averaged (Neuropack, Nihonkohden, Tokyo, Japan).

Immunohistochemistry

For immunohistochemistry, patient and normal sera (300 µl) were purified using the Melon Gel IgG purification kit according to the manufacturer's protocol (Pierce Biotechnology, Rockford, IL) to remove IgM, and purified sera were concentrated by Amicon Ultra 100 (Millipore, MA). The rhesus monkey eye cup was fixed with 4% paraformaldehyde in PBS for 30 min at 4°C. The samples were cryoprotected with 30% sucrose in PBS and embedded in OCT compound (Sakura Finetechnical, Tokyo, Japan). These tissues were sliced with a Microm HM 560 cryostat microtome (Microm Laborgeräte GmbH, Walldorf, Germany) into 14 µm. Sections were washed twice in PBS for 5 min, permeabilized with 0.1% Triton-X100/PBS, then washed with PBS 3 times for 5 min, and incubated with PBS containing 4% donkey serum for 1 hr to block samples. For the immunoreaction, the samples were incubated with a purified normal or CAR serum (1:300) diluted in blocking buffer at 4°C overnight. After PBS-washing, these samples were incubated with a DyLight-488 conjugated donkey anti-human IgG (H+L) (1:400) as a secondary antibody (Jackson Immunoresearch Laboratories) at room temperature for 1 hr and washed with PBS.

Transfection and Western blot analyses

HEK293T cells were cultured in D-MEM containing 10% fetal bovine serum (FBS; Nissui, Tokyo, Japan). These cells were grown under 5% carbon dioxide at 37°C. The calcium phosphate method was used to transfect the cells. Transfected cells were incubated at 37°C for 48 hrs, and then harvested for further analysis. The proteins extracted from the cells were separated by SDS–PAGE on a 7.5% precast gel (ATTO, Tokyo, Japan), and then transferred to a polyvinylidene difluoride membrane using the Invitrogen iBlot system (Invitrogen, Carlsbad, CA, USA). The membrane was incubated with primary antibodies, mouse anti-Flag (1:1,000; Sigma, St Louis, MO), sera from patients (1:100), normal human serum (1:100), or mouse anti-β-actin (1:5,000; Sigma). The membrane was then incubated with a horseradish peroxidase-conjugated goat anti-mouse IgG (1:10,000; Zymed Laboratories, San Francisco, CA) or donkey anti-human IgG (1:10,000; Jackson Immuno Research Laboratories, West Grove, PA) as secondary antibodies. The bands were developed using Chemi-Lumi One L (Nacalai Tesque, Kyoto, Japan).

Acknowledgments

We thank Richaed G. Weleber, Yozo Miyake, and Duco I. Hamasaki for helpful discussions of this study, Junko Hanaya for collecting the serum of our patients, and Mikiko Kadowaki, Aiko Ishimaru, Kaori Sone, and Shawna Kennedy for technical assistance.

Author Contributions

Conceived and designed the experiments: MK TF. Performed the experiments: MK RS SU YN NH. Analyzed the data: MK RS SU TF. Contributed reagents/materials/analysis tools: MK SU HO SY SM HT GA. Wrote the paper: MK TF. Supervised the project: MK HT TF.

References

1. Thirkill CE, FitzGerald P, Sergott RC, Roth AM, Tyler NK, et al. (1989) Cancer-associated retinopathy (CAR syndrome) with antibodies reacting with retinal, optic-nerve, and cancer cells. N Engl J Med 321: 1589–1594.
2. Chan JW (2003) Paraneoplastic retinopathies and optic neuropathies. Surv Ophthalmol 48: 12–38.
3. Heckenlively JR, Ferreyra HA (2008) Autoimmune retinopathy: A review and summary. Semin Immunopathol 30: 127–134.
4. Adamus G (2009) Autoantibody targets and their cancer relationship in the pathogenicity of paraneoplastic retinopathy. Autoimmun Rev 8: 410–414.

5. Thirkill CE, Roth AM, Keltner JL (1987) Cancer-associated retinopathy. Arch Ophthalmol 105: 372–375.
6. Jacobson DM, Thirkill CE, Tipping SJ (1990) A clinical triad to diagnose paraneoplastic retinopathy. Ann Neurol 28: 162–167.
7. Milam AH, Saari JC, Jacobson SG, Lubinski WP, Feun LG, et al. (1993) Autoantibodies against retinal bipolar cells in cutaneous melanoma-associated retinopathy. Invest Ophthalmol Vis Sci 34: 91–100.
8. Alexander KR, Fishman GA, Peachey NS, Marchese AL, Tso MOM (1992) "On" response defect in paraneoplastic night blindness with cutaneous malignant melanoma. Invest Ophthalmol Vis Sci 33: 477–483.
9. Lei B, Bush RA, Milam AH, Sieving PA (2000) Human melanoma-associated retinopathy (MAR) antibodies alter the retinal ON-response of the monkey ERG in vivo. Invest Ophthalmol Vis Sci 41: 262–266.
10. Lu Y, Jia L, He S, Hurley MC, Leys MJ, et al. (2009) Melanoma-associated retinopathy: a paraneoplastic autoimmune complication. Arch Ophthalmol 127: 1572–1580.
11. Jacobson DM, Adamus G (2001) Retinal anti-bipolar cell antibodies in a patient with paraneoplastic retinopathy and colon carcinoma. Am J Ophthalmol 131: 806–808.
12. Goetgebuer G, Kestelyn-Stevens AM, De Laey JJ, Kestelyn P, Leroy BP (2008) Cancer-associated retinopathy (CAR) with electronegative ERG: a case report. Doc Ophthalmol 116: 49–55.
13. Koike C, Obara T, Uriu Y, Numata T, Sanuki R, et al. (2010) TRPM1 is a component of the retinal ON bipolar cell transduction channel in the mGluR6 cascade. Proc Natl Acad Sci U S A 107: 332–337. Epub Dec. 4, 2009.
14. Koike C, Numata T, Ueda H, Mori Y, Furukawa T (2010) TRPM1: A vertebrate TRP channel responsible for retinal ON bipolar function. Cell Calcium 48: 95–101.
15. Morgans CW, Zhang J, Jeffrey BG, Nelson SM, Burke NS, et al. (2009) TRPM1 is required for the depolarizing light response in retinal ON-bipolar cells. Proc Natl Acad Sci U S A 106: 19174–19178.
16. Hartmann TB, Bazhin AV, Schadendorf D, Eichmüller SB (2005) SEREX identification of new tumor antigens linked to melanoma-associated retinopathy. Int J Cancer 114: 88–93.
17. Nakamura M, Sanuki R, Yasuma TR, Onishi A, Nishiguchi KM, et al. (2010) TRPM1 mutations are associated with the complete form of congenital stationary night blindness. Mol Vis 16: 425–437.
18. Li Z, Sergouniotis PI, Michaelides M, Mackay DS, Wright GA, et al. (2009) Recessive mutations of the gene TRPM1 abrogate ON bipolar cell function and cause complete congenital stationary night blindness in humans. Am J Hum Genet 85: 711–719.
19. van Genderen MM, Bijveld MM, Claassen YB, Florijn RJ, Pearring JN, et al. (2009) Mutations in TRPM1 are a common cause of complete congenital stationary night blindness. Am J Hum Genet 85: 730–736.
20. Audo I, Kohl S, Leroy BP, Munier FL, Guillonneau X, et al. (2009) TRPM1 is mutated in patients with autosomal-recessive complete congenital stationary night blindness. Am J Hum Genet 85: 720–729.
21. Miyake Y, Yagasaki K, Horiguchi M, Kawase Y, Kanda T (1986) Congenital stationary night blindness with negative electroretinogram: A new classification. Arch Ophthalmol 104: 1013–1020.
22. Bech-Hansen NT, Naylor MJ, Maybaum TA, Sparkes RL, Koop B, et al. (2000) Mutations in NYX, encoding the leucine-rich proteoglycan nyctalopin, cause X-linked complete congenital stationary night blindness. Nat Genet 26: 319–23.
23. Pusch CM, Zeitz C, Brandau O, Pesch K, Achatz H, et al. (2000) The complete form of X-linked congenital stationary night blindness is caused by mutations in a gene encoding a leucine-rich repeat protein. Nat Genet 26: 324–327.
24. Dryja TP, McGee TL, Berson EL, Fishman GA, Sandberg MA, et al. (2005) Night blindness and abnormal cone electroretinogram ON responses in patients with mutations in the GRM6 gene encoding mGluR6. Proc Natl Acad Sci USA 102: 4884–4889.
25. Miyake Y, Yagasaki K, Horiguchi M, Kawase Y (1987) On- and off-responses in photopic electroretinogram in complete and incomplete types of congenital stationary night blindness. Jpn J Ophthalmol 31: 81–87.
26. Houchin K, Purple RL, Wirtschafter JD (1991) X-linked congenital stationary night blindness and depolarizing bipolar system dysfunction. [ARVO abstract]. Invest Ophthalml Vis Sci 32: S1229.
27. Young RSL (1991) Low-frequency component of the photopic ERG in patients with X-linked congenital stationary night blindness. Clin Vis Sci 6: 309–315.
28. Khan NW, Kondo M, Hiriyanna KT, Jamison JA, Bush RA, et al. (2005) Primate retinal signaling pathways: Suppressing ON-pathway activity in monkey with glutamate analogues mimics human CSNB1-NYX genetic night blindness. J Neurophysiol 93: 481–492.
29. Polans AS, Witkowska D, Haley TL, Amundson D, Baizer L, et al. (1995) Recoverin, a photoreceptor-specific calcium-binding protein, is expressed by the tumor of a patient with cancer-associated retinopathy. Proc Natl Acad Sci U S A 92: 9176–9180.
30. Matsubara S, Yamaji Y, Sato M, Fujita J, Takahara J (1996) Expression of a photoreceptor protein, recoverin, as a cancer-associated retinopathy autoantigen in human lung cancer cell lines. Br J Cancer 74: 1419–1422.
31. Ohguro H, Odagiri H, Miyagawa Y, Ohguro I, Sasaki M, et al. (2004) Clinicopathological features of gastric cancer cases and aberrantly expressed recoverin. Tohoku J Exp Med 202: 213–219.
32. Bazhin AV, Schadendorf D, Willner N, De Smet C, Heinzelmann A, et al. (2007) Photoreceptor proteins as cancer-retina antigens. Int J Cancer 120: 1268–76.
33. Keltner JL, Thirkill CE (1999) The 22-kDa antigen in optic nerve and retinal diseases. J Neuroophthalmol 19: 71–83.
34. Potter MJ, Adamus G, Szabo SM, Lee R, Mohaseb K, et al. (2002) Autoantibodies to transducin in a patient with melanoma-associated retinopathy. Am J Ophthalmol 134: 128–30.
35. Shimazaki K, Jirawuthiworavong GV, Heckenlively JR, Gordon LK (2008) Frequency of anti-retinal antibodies in normal human serum. J Neuro-Ophthalmol 28: 5–11.

Toppan Best-set Premedia Limited
JOBNAME: 12503/black
Journal Code: CXO | Proofreader: Elsie
Article No: CXO796 | Delivery date: 30 Jul 2012
Page Extent: 6

CLINICAL AND EXPERIMENTAL
OPTOMETRY

RESEARCH PAPER

Low luminance visual acuity in patients with central serous chorioretinopathy

Clin Exp Optom 2012 DOI:10.1111/j.1444-0938.2012.00796.x

Kyoko Fujita* MD PhD
Kei Shinoda† MD PhD
Celso Soiti Matsumoto† MD PhD
Yutaka Imamura§ MD PhD
Yoshihiro Mizutani* MD, PhD
Etsuko Tanaka‖ PhD
Atsushi Mizota† MD, PhD
Koichi Oda¶ PhD
Mitsuko Yuzawa* MD PhD

* Department of Ophthalmology, Surugadai Nihon University Hospital, Tokyo, Japan
† Department of Ophthalmology, Teikyo University School of Medicine, University Hospital Itabashi, Tokyo, Japan
§ Department of Ophthalmology, Teikyo University School of Medicine, University Hospital Mizonokuchi, Kanagawa, Japan
‖ Department of Ophthalmology, Kyorin University School of Medicine, Tokyo, Japan
¶ Department of Communication, Tokyo Women's Christian University, Tokyo, Japan
E-mail: shinodak@med.teikyo-u.ac.jp

Submitted: 25 January 2012
Revised: 25 May 2012 Accepted for publication: 4 June 2012

Background: The aim was to determine the low luminance visual acuity in eyes with central serous chorioretinopathy.

Methods: Seven eyes of seven patients with central serous chorioretinopathy and six eyes of six age-matched normal volunteers were examined. Low luminance visual acuity charts were created by an Apple Power Mac G5 computer and displayed on a cathode ray tube monitor (SONY GDM-F500). The background luminance was set at six different levels from 78.20 cd/m^2 to 0.37 cd/m^2. The visual acuities of the eyes with central serous chorioretinopathy at each of the six luminance levels were compared to those from their fellow eyes and to normal eyes.

Results: The mean visual acuities varied from 0.13, 0.23, 0.29, 0.42, 0.62 to 0.70 logMAR units as luminance varied from high to low. At the lowest luminance (0.37 cd/m^2), five of the seven eyes could not read any character. The mean visual acuities of the fellow eyes at the same luminance levels were 0.03, 0.06, 0.11, 0.20, 0.27 and 0.45 logMAR units and those of the normal volunteers were 0, 0.03, 0.08, 0.14, 0.23 and 0.38 logMAR units, respectively. The visual acuities of the eyes with central serous chorioretinopathy were significantly poorer than those of the normal eyes at all luminance levels except 0.37 cd/m^2 ($p < 0.05$ for all).

Conclusions: Although the eyes from all three groups had 0 logMAR units visual acuity under standard testing condition, the visual acuity of the eyes with central serous chorioretinopathy were significantly worse at low luminance levels. The low luminance visual acuity may provide information on the visual disturbances reported by central serous chorioretinopathy patients with 0 logMAR units visual acuity.

Key words: central serous chorioretinopathy, contrast sensitivity, low luminance visual acuity, optical coherence tomography, serous retinal detachment

Central serous chorioretinopathy (CSC) is characterised by a serous retinal detachment in the macular area. Central serous chorioretinopathy patients range in age from 20 to 50 years but most are middle-aged men. The central serous chorioretinopathy causes a central and paracentral relative scotoma in the visual field.[1–3] Although the visual acuity (VA) is relatively good, patients often complain of difficulty with visual activities performed in the evening and at night under low ambient illumination. In conventional VA tests, such visual disturbances are usually not detected because the backgrounds of VA testing charts have high luminance.

To evaluate patients with central serous chorioretinopathy and visual disturbances

under low luminance conditions, we need to measure the VA using test charts with low background luminance. It is well known that VA is affected by the degree of ambient luminance and Shaler[4] reported that the VA of normal eyes decreased under low luminance conditions. Because patients with good VA can have depressed visual function, for example, decreased contrast sensitivity, poorer colour discrimination, reduced focal macular electroretinogram (ERG), reduced focal retinal sensitivity and visual field defects,[5–12] it might be expected that patients with central serous chorioretinopathy would also have decreased VA under low luminance. There have been no studies focusing on low luminance VA in patients with central serous chorioretinopathy.

The purpose of this study was to determine the VA of patients with central serous chorioretinopathy under low luminance conditions. To accomplish this, we made a computer program to create low luminance visual acuity charts and determined the VA under six different background luminance levels in seven patients with central serous chorioretinopathy.

METHODS

Seven eyes of seven patients with central serous chorioretinopathy and six eyes of six age-matched healthy control subjects were tested. The inclusion criteria were:

1. presence of subretinal fluid (serous retinal detachment: SRD) involving the fovea in the optical coherence tomographic (OCT) images
2. unilateral central serous chorioretinopathy with the fellow eye normal and
3. visual acuity of 0 logMAR or better in both eyes.

The exclusion criteria were:

1. evidence of choroidal neovascularisation in the fluorescein angiographic (FA) and indocyanine green angiographic images and
2. the presence of other ocular or macular diseases. Patients with central serous chorioretinopathy, who had received laser photocoagulation were also excluded.

The diagnosis of central serous chorioretinopathy was based on the presence of a serous retinal detachment documented by leakage from the retinal pigment epithelium in the fluorescein angiographic images. The VA was measured with a Landolt C chart using standard retroillumination with a luminance of 220 cd/m^2. We also examined six eyes of six normal volunteers with the same testing protocol. The OCT examination was carried out with either a Heidelberg Spectralis OCT (Heidelberg Engineering, Heidelberg, Germany) or with a Stratus OCT 3000 (Carl Zeiss Meditec, Inc, Dublin, CA, USA). The height of the serous retinal detachment (SRDH), the width of the serous retinal detachment (SRDW) and the thickness of sensory retina (foveal thickness: FT) were manually measured in the horizontal cross-sectional OCT images, which included the fovea (Figure 1). These measurements were made by one of the authors (KS), who had no information about the patients. The values of these parameters were used for statistical analyses.

The procedures used in this study conformed to the tenets of the Declaration of Helsinki. An informed consent was obtained from all subjects. Approval to conduct this study was obtained from the Institutional Review Board of Surugadai Nihon University Hospital, Tokyo, Japan.

Low luminance visual acuity charts and procedures

Low luminance VA charts were created with an Apple PowerMac G5 computer and displayed on a monitor (SONY GDM-F500). Landolt Cs were used for the characters and they followed the design rule of the Early Treatment Diabetic Retinopathy Study charts (Figure 2). Six levels of background luminance were used, namely, 78.20 cd/m^2, 31.87 cd/m^2, 11.37 cd/m^2, 4.14 cd/m^2, 1.30 cd/m^2 and 0.37 cd/m^2. The luminance of the Landolt C rings was kept as close to zero cd/m^2 as possible and the contrast for all conditions approached 100 per cent.

Identification of the largest Landolt C at the distance of 308 cm represented a VA of 0.7 logMAR units. The ring size was reduced in steps of 0.1 to -0.4 logMAR units. The tests were conducted from the lowest luminance level in a dark room after waiting seven minutes for dark adaptation.

Analyses

We compared the VA of the eyes with central serous chorioretinopathy with that of the fellow eyes and that of normal eyes at each luminance level. To determine the statistical significance of any differences, Student's *t*-tests were used. The VA in logMAR units was plotted on the ordinate for the different luminance levels on the abscissa. The data were fit to a linear equation as:

$$y = a * x + b,$$

where 'y' is the logMAR VA and 'x' is the luminance expressed in logarithmic units. 'a' is the steepness of the best-fitted line and represents how much the VA is altered by a step change in the background luminance.

Thus, a large 'a' value means that the VA would be greatly changed by a step change in the background luminance. 'b' is the logMAR VA at very low or no background luminance, that is, when 'x' is zero. This is the point where the regression line intersects the ordinate of the logMAR VA line (Figure 1). The difference in the slopes for central serous chorioretinopathy, fellow and normal eyes were tested for significance by assessing the interaction term between background luminance and eye type using an analysis of covariance (ANCOVA) technique.

The correlations between the parameters of the OCT images and the constants 'a' and 'b' were determined by the Spearmann coefficients of correlation. The Bonferroni correlation was used to avoid type I error. The statistical significance was set at 0.01 for the *t*-tests because there were five comparisons and at 0.17 for the ANCOVA because there were three comparisons.

RESULTS

The patients with central serous chorioretinopathy included five men and two women and the mean and standard deviation of their ages was 41.3 ± 3.9 years (range 39–50 years). The duration of the

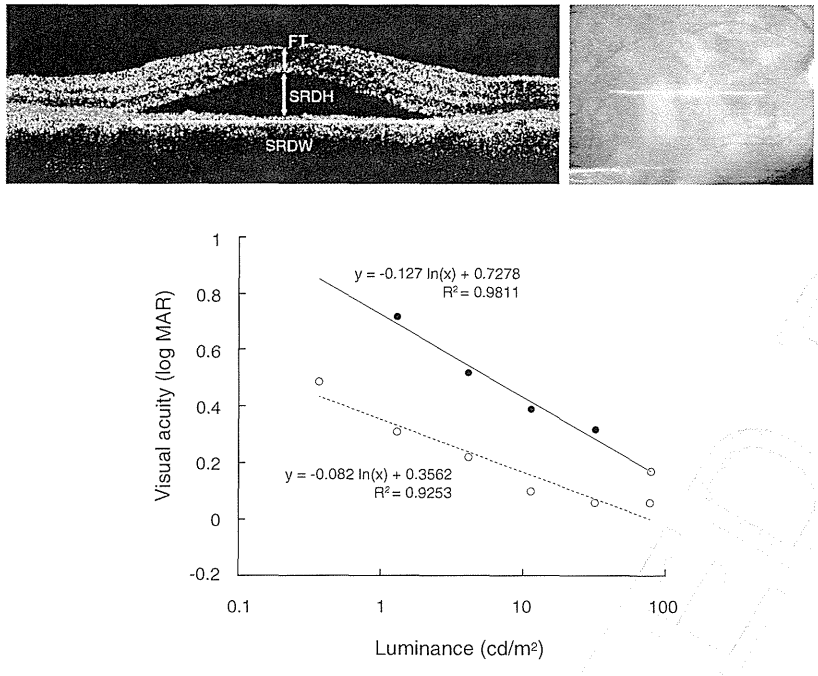

Colour

Figure 1. Optical coherence tomographic (OCT) image and infrared fundus photograph; also shown in a graph relating the visual acuity in logMAR units to the background luminance in eyes with central serous chorioretinopathy (CSC). The serous retinal detachment height (SRDH) was taken to be the distance between the outer segment/inner segment (IS/OS) line of the photoreceptors and the anterior surface of the retinal pigment epithelium/Bruch membrane. The width of the serous retinal detachment (SRDW) was taken to be the width of the serous retinal detachment in the OCT images and the foveal thickness was the distance between the internal limiting membrane (ILM) and IS/OS line. In cases where the IS/OS line was not clear, the basal edge of the hyper-reflective band representing the detached sensory retina was used.
Top left: Horizontal cross-sectional optical coherence tomographic (OCT) image including the fovea in an eye with central serous chorioretinopathy (Case 5). The cross-section corresponds to the horizontal line indicated in the right side of the fundus photograph. The serous retinal detachment height (SRDH), width of the serous retinal detachment (SRDW) and the foveal thickness (FT) are shown.
Top right: Infrared fundus photograph indicating the cross line of the left-side OCT image.
***Bottom*: Relationship between logMAR visual acuity (VA) and background luminance in Case 5. The logMAR VA was linearly correlated with the luminance. The logMAR VA of the central serous chorioretinopathy-affected eye was higher than that of the healthy fellow eye at each luminance level. ●: affected eye, ○: healthy fellow eye. The fitted line and the formula are shown as well.**

symptoms was 1.0–1.5 months (Table 1). The mean ages of the normal volunteers was 38 ± 9 years (range 22–47 years). The mean VAs of the central serous chorioretinopathy and fellow eyes at each luminance are shown in Table 1. At the lowest luminance level of 0.37 cd/m^2, five of seven patients could not correctly identify any of the targets using the eye with central serous chorioretinopathy. The mean VAs of the normal volunteers were 0 ± 0.05, 0.03 ± 0.04, 0.07 ± 0.06, 0.14 ± 0.06, 0.23 ± 0.11 and 0.38 ± 0.11 logMAR units, respectively.

The VA in logMAR units is plotted against the background log luminance in Figure 3. The VA of the eyes with central serous chorioretinopathy was significantly poorer than that of normal eyes at all luminances except 0.37 cd/m^2 and 78.20 cd/m^2 ($p < 0.01$ for all). The VA of the eyes with central serous chorioretinopathy was significantly poorer than that of fellow eyes at all luminances except 0.37 cd/m^2 and 78.20 cd/m^2 ($p < 0.01$ for all). No significant differences were found among the central serous chorioretinopathy, fellow and volunteer eyes in the slopes of the fitted linear function by ANCOVA.

The constants, 'a' and 'b' and the coefficient of regression (R^2) are shown in Table 2. There was no significant correlation between any OCT parameters and 'a' (slope) or 'b' (intercept).

DISCUSSION

Patients with central serous chorioretinopathy have a relatively central scotoma, metamorphopsia, micropsia, colour vision abnormalities, and visual disturbances under low luminance despite the relatively good standard VA. Studies on the relationship between the luminance of the VA charts and VA in eyes with central serous chorioretinopathy have not been reported. Patients with central serous chorioretinopathy often complain of difficulty in reading during the evening and night, that is, at low luminance levels. The VA obtained by conventional acuity charts is not a good measure for predicting how these patients will perform in low luminance environments.